Development of Driver Posture Prediction and Accommodation Models for Military Vehicles: Fixed-Eye-Point, Out-of-Hatch, and Highly Reclined Driver Configurations

Matthew P. Reed
Sheila M. Ebert

University of Michigan Transportation Research Institute

Final Report

UMTRI-2020-5

February 2020

Technical Report Documentation Page

1. Report No. UMTRI-2020-5	2. Government Accession No.	3. Recipient's Catalog No.
4. Title Development of Driver Posture Prediction and Accommodation Models for Military Vehicles: Fixed-Eye-Point, Out-of-Hatch, and Highly Reclined Driver Configurations		5. Report Date 6. Performing Organization Code
7. Author(s) Reed, M.P. and Ebert, S.M.		8. Performing Organization Report No. UMTRI-2020-5
9. Performing Organization Name and Address University of Michigan Transportation Research Institute 2901 Baxter Rd. Ann Arbor MI 48109		10. Work Unit No. (TRAIS) 11. Contract or Grant No.
12. Sponsoring Agency Name and Address		13. Type of Report and Period Covered 14. Sponsoring Agency Code
15. Supplementary Notes		

16. Abstract

Accurate information on warfighter posture and position is essential for the design of military vehicles for safety and effectiveness. In prior work, posture measurements from soldiers were used to develop statistical posture-prediction and accommodation models for drivers in fixed-heel-point configurations and fixed-position squad seats. In the current study in the series, soldiers were measured in mockups of three driver seating configurations: fixed eye point, out of hatch, and highly reclined. In each configuration, soldiers adjusted certain components to obtain a comfortable driving posture, which was measured by recording the three-dimensional locations of body landmarks. Data were gathered with three ensembles: advanced combat uniform (ACU), body armor vest and helmet (PPE level), and with the addition of a simulated rifleman kit. Internal joint center locations were estimated from surface landmarks. Statistical posture-prediction models were developed using regression analysis to predict the locations of important landmarks, such as the hip joint centers, eyes, and knees. Population accommodation models were developed using standard parametric techniques. These models generate surface contours that can be used in design to accommodate a desired percentage of a vehicle occupant population. The models take into account the effects of population anthropometry, clothing and gear ensemble, and vehicle configuration. Contours were generated for eye location, seat position, pedal location, steering yoke location, helmet clearance, elbow clearance, knee clearance, and torso clearance.

17. Key Word anthropometry, vehicle seats, posture, seat index point, H-point, human accommodation reference point	18. Distribution Statement		
19. Security Classif. (of this report) DIST A: Public Release	20. Security Classif. (of this page)	21. No. of Pages 74	22. Price

Form DOT F 1700.7 (8-72) Reproduction of completed page authorized

Metric Conversion Chart

APPROXIMATE CONVERSIONS TO SI UNITS

SYMBOL	WHEN YOU KNOW	MULTIPLY BY	TO FIND	SYMBOL
LENGTH				
In	inches	25.4	millimeters	mm
Ft	feet	0.305	meters	m
Yd	yards	0.914	meters	m
Mi	miles	1.61	kilometers	km
AREA				
in^2	squareinches	645.2	square millimeters	mm^2
ft^2	squarefeet	0.093	square meters	m^2
yd^2	square yard	0.836	square meters	m^2
Ac	acres	0.405	hectares	ha
mi^2	square miles	2.59	square kilometers	km^2
VOLUME				
fl oz	fluid ounces	29.57	milliliters	mL
gal	gallons	3.785	liters	L
ft^3	cubic feet	0.028	cubic meters	m^3
yd^3	cubic yards	0.765	cubic meters	m^3
NOTE: volumes greater than 1000 L shall be shown in m^3				
MASS				
oz	ounces	28.35	grams	g
lb	pounds	0.454	kilograms	kg
T	short tons (2000 lb)	0.907	megagrams (or "metric ton")	Mg (or "t")
TEMPERATURE (exact degrees)				
ºF	Fahrenheit	5 (F-32)/9 or (F-32)/1.8	Celsius	ºC
FORCE and PRESSURE or STRESS				
lbf	poundforce	4.45	newtons	N

lbf/in^2	poundforce per square inch	6.89	kilopascals	kPa
LENGTH				
mm	millimeters	0.039	inches	in
m	meters	3.28	feet	ft
m	meters	1.09	yards	yd
km	kilometers	0.621	miles	mi
AREA				
mm^2	square millimeters	0.0016	square inches	in^2
m^2	square meters	10.764	square feet	ft^2
m^2	square meters	1.195	square yards	yd^2
ha	hectares	2.47	acres	ac
km^2	square kilometers	0.386	square miles	mi^2
VOLUME				
mL	milliliters	0.034	fluid ounces	fl oz
L	liters	0.264	gallons	gal
m^3	cubic meters	35.314	cubic feet	ft^3
m^3	cubic meters	1.307	cubic yards	yd^3
MASS				
g	grams	0.035	ounces	oz
kg	kilograms	2.202	pounds	lb
Mg (or "t")	megagrams (or "metric ton")	1.103	short tons (2000 lb)	T
TEMPERATURE (exact degrees)				
ºC	Celsius	1.8C+32	Fahrenheit	ºF
FORCE and PRESSURE or STRESS				
N	Newtons	0.225	poundforce	lbf
kPa	Kilopascals	0.145	poundforce per square inch	lbf/in^2

*SI is the symbol for the International System of Units. Appropriate rounding should be made to comply with Section 4 of ASTM E380.
(Revised March 2003)

ACKNOWLEDGMENTS

This research was supported by the Automotive Research Center (ARC) at the University of Michigan under agreement W56H2V-14-2-0001 with the US Army Tank Automotive Research, Development, and Engineering Center (TARDEC) in Warren, MI. We thank our colleagues Gale Zielinski and Frank Huston of the Ground Vehicle Systems Center, who collaborated on all aspects of the project. We also thank Bruce Bradtmiller, Michael Mucher, and Patricia Barrientos from Anthrotech for their assistance with data collection. Our data collection would not have been possible without the generous assistance of Fred Corbin and the Soldier volunteers at Fort Hood.

CONTENTS

ABSTRACT

Accurate information on warfighter posture and position is essential for the design of military vehicles for safety and effectiveness. In prior work, posture measurements from Soldiers were used to develop statistical posture-prediction and accommodation models for drivers in fixed-heel point configurations and fixed-position squad seats. In the current study in the series, Soldiers were measured in mockups of three driver seating configurations: fixed eye point, out of hatch, and highly reclined. In each configuration, Soldiers adjusted certain components to obtain a comfortable driving posture, which was measured by recording the three-dimensional locations of body landmarks. Data were gathered with three ensembles: advanced combat uniform (ACU), body armor vest and helmet (PPE level), and with the addition of a simulated rifleman kit. Internal joint center locations were estimated from surface landmarks. Statistical posture-prediction models were developed using regression analysis to predict the locations of important landmarks, such as the hip joint centers, eyes, and knees. Population accommodation models were developed using standard parametric techniques. These models generate surface contours that can be used in design to accommodate a desired percentage of a vehicle occupant population. The models take into account the effects of population anthropometry, clothing and gear ensemble, and vehicle configuration. Contours were generated for eye location, seat position, pedal location, steering yoke location, helmet clearance, elbow clearance, knee clearance, and torso clearance.

INTRODUCTION

Driver accommodation models provide quantitative guidance for vehicle design by predicting the distribution of driver-selected seat position and eye location, among other variables. Designers use these models to select component adjustment ranges that accommodate a large percentage of drivers and to ensure visibility within and outside of the vehicle.

This report is one of a series documenting research to develop modern human-centered design tools for military vehicles. For each project, we have gathered posture, position, and adjustment data from Soldiers sitting in mockups of vehicle interior environments. The data are analyzed to develop statistical models predicting posture and accommodation requirements for individuals and populations as a function of Soldier and vehicle characteristics.

The current report focuses on driver workstations with three configurations: a fixed eye point, an out-of-hatch posture with a high seat height, and highly reclined postures. Most conventional vehicle designs have fixed pedals and a highly adjustable seat, possibly with an adjustable steering wheel. These fixed-heel workstations were addressed previously (Zerehsaz et al. 2014a). Fixed-eye-point (FEP) designs are increasingly relevant for scenarios in which drivers are fully under armor, driving using optical systems (e.g., periscopes) or camera-based systems with screen displays. Out-of-hatch (OOH) postures are used in low-threat conditions when high levels of exterior vision are beneficial. OOH conditions are typically encountered in adaptable driving positions that also include a fixed-heel or fixed-eye driving condition. Highly reclined seating (HRS) is relevant for some current combat vehicles and may be increasingly relevant for driving configurations in other vehicles that are fully under-armor.

The data for the current study were gathered from Soldiers at Fort Hood, Texas. Trained investigators obtained standard anthropometric dimensions and measured body landmark locations as the Soldiers sat in a range of configurations in each mockup. The data were analyzed using statistical techniques developed in earlier work to produce posture-prediction and population accommodation models. The posture-prediction models give the most likely component adjustments, body landmark locations, and segment orientations as function of Soldier body dimensions and the vehicle layout. These models are used to posture human figure models that represent Soldiers of specific sizes. The population accommodation models are based on the same analysis but incorporate the population variance to produce statistical representations of the boundaries of Soldier preferences for component adjustment ranges as well as space claim for the head, torso, knees, and elbows. Population accommodation models are used to assess current designs and as design guidance for future vehicles.

METHODS

Human Research Approval

The study protocol was approved by a University of Michigan Institutional Review Board and by the USAMRMC Office of Research Protections Human Research Protection Office (HRPO). Written informed consent was obtained from each participant.

Data Collection Site

The Army provided access to facilities at Fort Hood, Texas. The equipment, which was developed and fitted at UMTRI, was shipped to the base and set up by UMTRI and Anthrotech staff. Data collection was conducted September through November 2014. Soldiers were invited to participate by local personnel at each base. By design, the subject pool was not recruited to match a particular profile. Rather this convenience sample was intended to provide a broad range of human variability that is not necessarily representative of any particular part of the Army. The analysis methods enable the results to be tailored to any desired component of the current or future Army.

Standard Anthropometry

Anthropometric data were gathered from each Soldier to characterize overall body size and shape following the procedures documented in Hotzman et al. (2011) for the ANSUR II survey. Standard anthropometric measures were obtained using manual measurements. The measurements included the core subset of dimensions gathered in ANSUR II. Table 1 lists the dimensions along with their corresponding identification in ANSUR II. All measurements were obtained with the Soldiers wearing their PT shorts, except that stature was measured with and without boots to characterize heel height. Tables 2-4 list summary statistics for selected anthropometric dimensions for Soldiers measured in each of the three mockups.

Table 1
Standard Anthropometric Measures

	Measurement	Posture	ANSUR II
1	Weight		6.4.92
2	Tragion to Top of Head	Sitting	6.4.83
3	Head Length	Sitting	6.4.48
4	Head Breadth	Sitting	6.4.46
5	Erect Sitting Height	Sitting	6.4.72
6	Eye Height	Sitting	6.4.35
7	Acromial Height	Sitting	6.4.2 (standing)
8	Knee Height	Sitting	6.4.58
9	Popliteal Height	Sitting	6.4.67
10	Acromial Breadth	Sitting	6.4.9
11	Bideltoid Breadth	Sitting	6.4.12
12	Maximum Hip Breadth	Sitting	6.4.52
13	Buttock-Knee Length	Sitting	6.4.20
14	Buttock-Popliteal Length	Sitting	6.4.21
15	Acromion – Radiale Length	*Sitting*	6.4.3 (standing)
16	Forearm – Hand Length	*Sitting*	6.4.41 (standing)
17	Stature Without Boots	Standing	6.4.76
18	Stature With Boots	Standing	
19	Chest Circumference (max anterior pt)	Standing	6.4.25
20	Waist Circumference at Omphalion	Standing	6.4.88
21	Hip Circumference at Buttocks	Standing	6.4.17
22	Bispinous Breadth	Standing	

Table 2
Anthropometry Summary, Fixed-Eye-Point (60 men, 19 women)

Variable	Min	Mean	SD	Max
Stature	1519	1712	93.3	1941
Weight (kg)	43.9	76.8	15.1	128.8
BMI (kg/m2)	19	26.0	3.5	35.8
Age (yr)	19	24.1	4.4	39

Table 3
Anthropometry Summary, Out-of-Hatch (37 men, 12 women)

Variable	Min	Mean	SD	Max
Stature	1519	1708	77.0	1849
Weight (kg)	43.9	76.9	13.6	111.7
BMI (kg/m2)	19	26.3	3.7	33.7
Age (yr)	19	24.3	4.6	39

Table 4
Anthropometry Summary, Highly Reclined Seating (41 men, 12 women)

Variable	Min	Mean	SD	Max
Stature	1542	1711.6	84.1	1918
Weight (kg)	49.3	77.0	15.4	128.8
BMI (kg/m2)	20.3	26.1	4.0	35.8
Age (yr)	19	23.9	4.4	39

Ensemble Levels and Fitting

Testing was conducted in three ensemble levels selected to be the same as those used in the earlier study with fixed-heel-point conditions. Figure 1 shows the three ensemble levels. At the ACU level, Soldiers wore their own advanced combat uniform consisting of a jacket, trousers, moisture wicking shirt and brown combat boots. All items were removed from the pockets, extra padding removed from the knees, and any cap or helmet removed. At the PPE (personal protective equipment) level, Soldiers wore an Improved Outer Tactical Vest (IOTV) with Enhanced Small Arms Protective Insert (ESAPI) plates, Enhanced Side Ballistic Inserts (ESBI), and an Advanced Combat Helmet (ACH) over their ACU ensemble. Five sizes of IOTV were available at the study site. Examples are shown in Figures 2-4. The Soldiers were given their self-reported sizes of helmet and IOTV with front, back and side plates. The investigator helped the Soldier don the PPE and checked the fit. The fit was considered acceptable if (1) the elastic waistband of the IOTV was snug with the Velcro closure fully overlapped and (2) the bottom of the IOTV was located below the navel and above the belt. The Soldiers wore the smallest size helmet in which the Soldier's head was in contact with the padding on the inside of the top of the helmet.

The third level of gear was referred to as body-born gear (BBG) or encumbered (ENC), which consisted of ACU, PPE, a hydration pack, and a Tactical Assault Panel (TAP). Note that BBG/ENC is nominally identical to the rifleman ENC condition used in the earlier study.

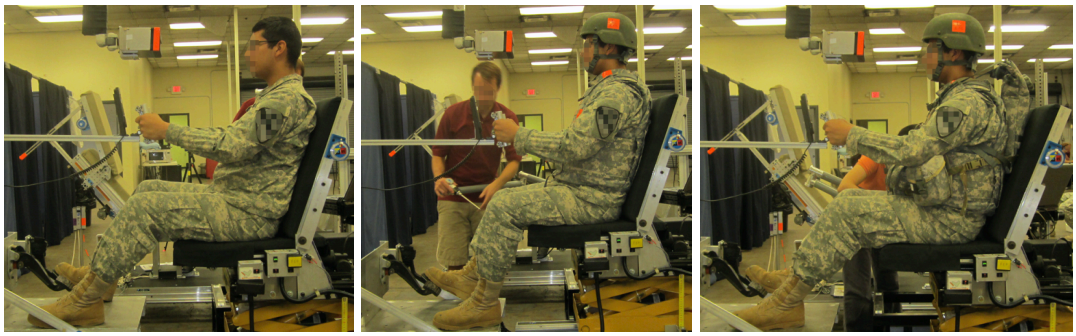

Figure 1. The three ensemble levels, from left: ACU, PPE, and BBG (ENC).

The TAP is an adaptable platform intended to replace the Fighting Load Carrier (FLC) vest to allow for quick release of equipment in emergency situations (Figures 5 and 6). The TAP is designed to carry a variety of basic Modular Lightweight Load-Carrying Equipment (MOLLE) fighting load pouches. The TAP was equipped with a harness that went over the head and around the sides. A CamelBak-style hydration system (Figure 5), filled with 2.5 L of water, was attached to the back. The rifleman's TAP represents the load of a rifleman or driver of a transport vehicle. This ensemble includes a communications radio. Table 5 lists the items carried in the TAP. Targets were applied to the helmet and IOTV to facilitate tracking during testing (Figures 7 and 8). The locations of these targets were recorded in trials in which this gear was present.

Figure 2. Soldier in his ACU selecting IOTV

Figure 3. Testing IOTV fit and Soldier tightening ACH and checking size

Figure 4. Participant in BBG (ENC) ensemble.

Figure 5. TAP and hydration close up

Figure 6. TAP laid flat.

Table 5
Inventory of Equipment in Rifleman BBG (ENC)

Item	Count
Replica M16 magazine clips	8
Replica Multiband Inter/Intra Team Radio (MBITR)	1
Replica fragmentation grenade	2
Multipliers	1
Canteen case with weight of night vision goggles added	1
Improved first aid kit (IFAK)	1
TAP with pouches	1

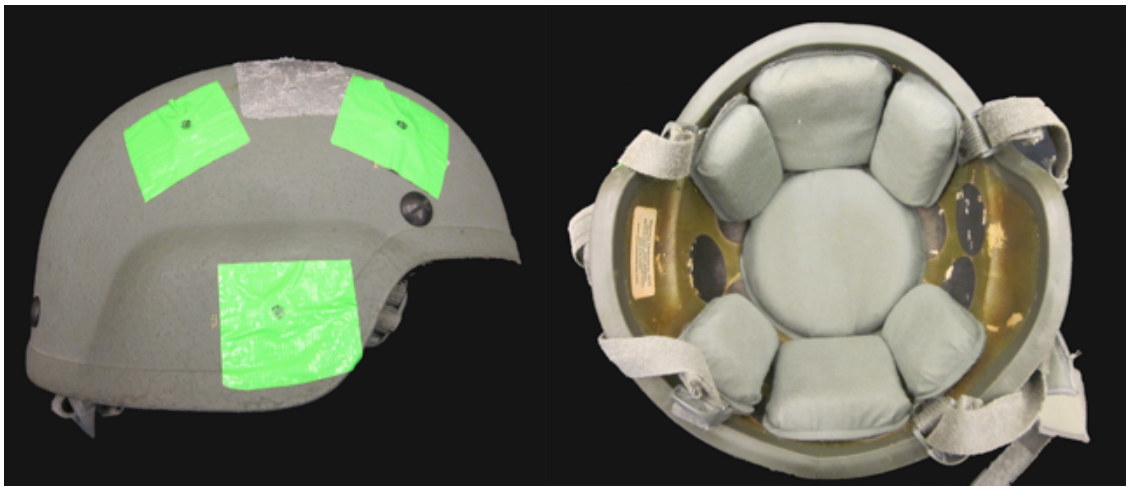

Figure 7. ACH with reference points and interior with pads configuration tested

Figure 8. IOTV with reference points

Participant Interaction Scripts

Appendix A lists the participant interaction scripts for each mockup. These interaction scripts ensured that each participant received the same information and instructions.

Mockups and Test Conditions

Fixed Eye Point (FEP)

The mockup shown in Figure 9 was fabricated for this data collection. The vertical and horizontal seat position was adjustable using motorized controls. The seat back angle could also be adjusted, and the seat cushion angle was fixed at 6 degrees (SAE A27). The floor height was set to three different levels, depending on the test condition (see below). The pedal and floor assembly could be moved fore-aft with a motorized control. A steering yoke was mounted on a motorized support that could be moved fore-aft and vertically.

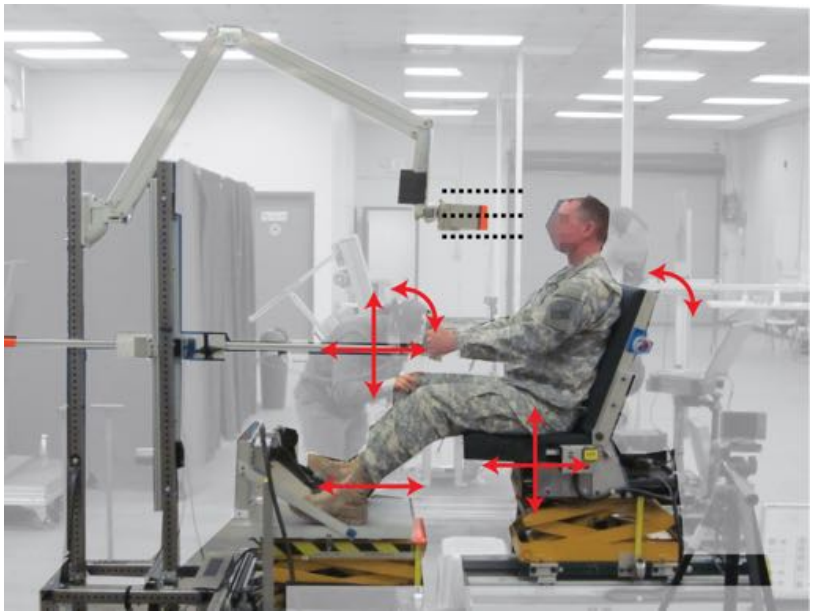

Figure 9. FEP mockup. Red arrows show motorized adjustment ranges available to participant.

The seat Human Accommodation Reference Point (HARP) was measured using the SAE J826 H-point machine (Figure 10). Note that the seat back angle in the mockup seat is taken to be equal to be the angle of the undeflected surface of the seat back with respect to vertical, which is equivalent to the H-point manikin torso angle when installed at midrange positions. The HARP was measured with the seat back angle at 17 degrees.

Figure 10. Measuring the Human Accommodation Reference Point location in the FEP seat with the SAE J826 H-point machine.

The mockup was intended to simulate a situation in which the driver of a military ground vehicle needed to adjust the seat to attain an eye location in a narrow zone, such as when driving with an indirect vision system. Such a system was simulated by using a rectangular box shown in Figures 11 and 12. The front of the box (toward the subject) was partially open so that the subject could see through to the back of the box. When the participant was in the correct fore-aft and vertical position, the lines on the back of the box were lined up with the edges of the front opening. Figure 12 shows the instructions to the subject. Participants adjusted the seat position (fore-aft and vertical) and seat back angle to place their eyes in the correct location.

Figure 11. Soldier positioning himself to the FEP.

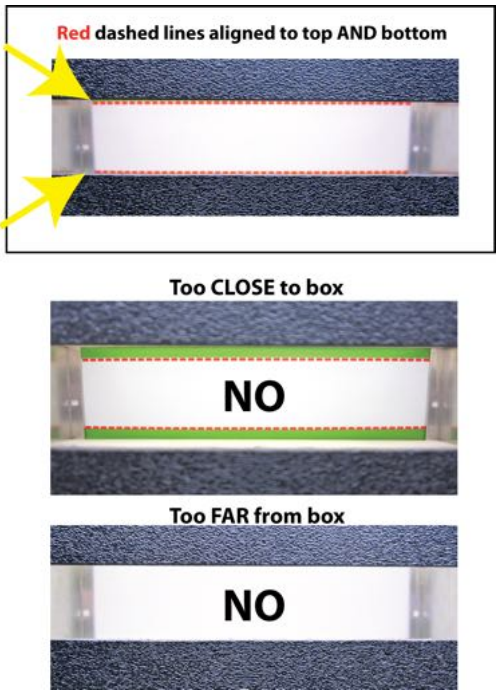

Figure 12. Illustration to subjects for obtaining proper alignment to FEP fixture.

Table 6 lists the five test conditions with FEP, which were differentiated by the FEP height above the floor and gear (ensemble) level. The FEP height above the floor was set to produce a range of seat heights for each subject. Because the vertical offset between the seat and the eye is strongly determined by body size, using fixed FEP heights above the floor would mean that taller subjects would experience lower seat heights. To ensure that all subjects experienced a similar range of seat heights, and to permit the testing to be conducted with a relatively narrow range of both seat and floor height adjustment, a posture prediction model from an earlier study (Reed and Ebert 2013) was used to choose the low, medium, and high FEP settings for each subject.

Table 6
FEP Condition Matrix

Condition Number	FEP Height Above Floor	Gear Level
C02	Med	BBG (ENC)
C09	Med	PPE
C10	Low	PPE
C11	High	PPE
C16	Med	ACU

The test conditions targeted a nominal seat height (HARP above heel) of 300, 425, and 550 mm. The eye height above HARP was predicted from the subject's body dimensions as:

$$EyeReHARPZ = -816 + 0.411*Stature+29*\ln(BMI)+1262*SH/S$$

where Stature is erect standing height in mm, ln(BMI) is the natural log of the body mass index (body mass in kg divided by stature in meters squared), and SH/S is the ratio of erect sitting height to stature. [Note that this equation was used to set test conditions and is not an outcome of the current study.]

A typical value of EyeReHARPZ for a midsize male is 654 mm. This value was added to the target seat height for each condition to obtain the desired FEP above AHP. These values were achieved by both changing the height of the heel surface and raising or lowering the eye box (see Figures 13 and 14).

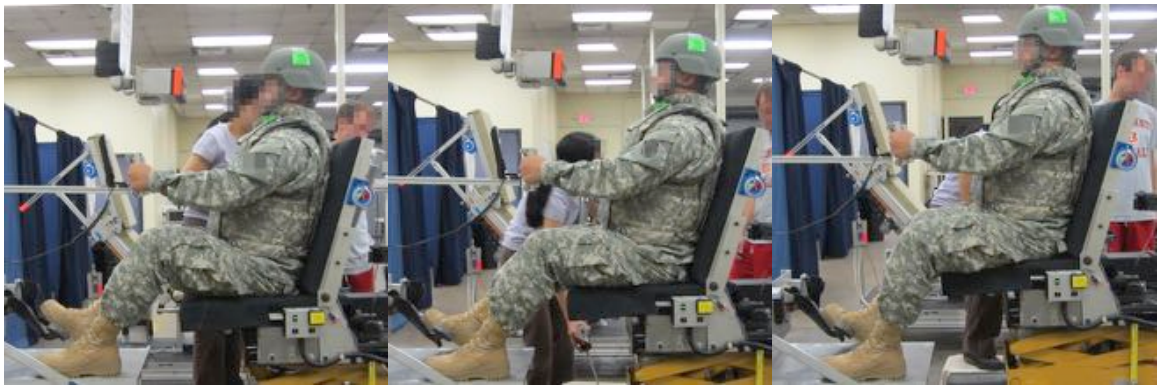

Figure 13. FEP at three settings of FEP above the floor, from left: low (C10), mid (C09), high (C11)

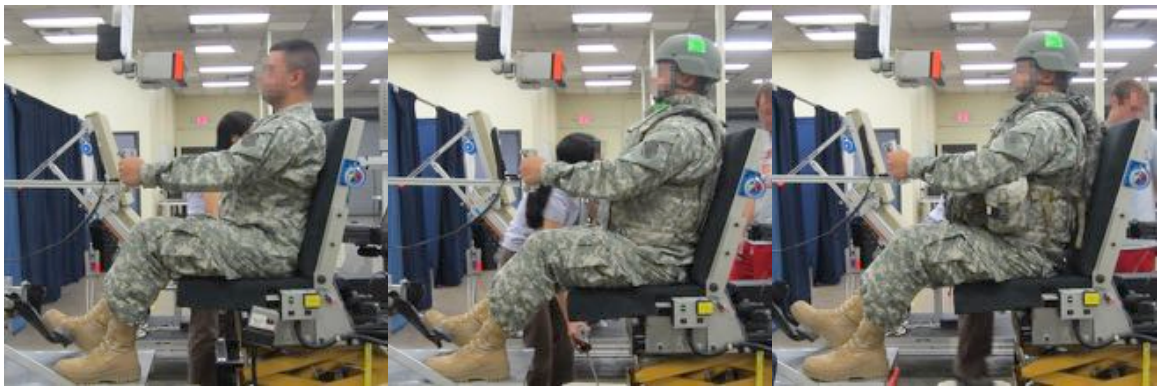

Figure 14. FEP set to mid height at three ensemble levels, from left: ACU (C16), PPE (C09), and ENC (C02)

Out of Hatch (OOH)

The FEP mockup was adapted for the OOH configurations. The goal in these conditions was to obtain data on postures for Soldiers sitting on a high seat with their torsos essentially upright. To obtain a sufficient range of postures for all participants, the seat

height was adjusted based on each participant's body dimensions, according to these equations:

Effective Leg Length (LL) = Stature without shoes – erect sitting height

Mid seat height (LP) = 0.95 * LL

Lower seat height (LP- offset) = 0.878 * LL

Higher seat height (LP- offset) = 1.022 * LL

The seat back angle was set to 5 degrees (fixed) for all OOH conditions. Testing was conducted at three seat heights with PPE and only at the middle seat height (LP) with ACU and ENC (Table 7). The steering yoke was fully adjustable up/down/tilt, and the position of the yoke was an outcome measure as in the other driving configurations in this study. In addition to the Soldier-selected (preferred) yoke position, the Soldier also demonstrated the lowest comfortable position for the yoke (Figure 15). After the participant had selected a comfortable driving posture with the steering yoke, the investigator interactively placed a "pedal" block at the Soldier's preferred right-foot position to simulate an accelerator pedal. Figures 16 and 17 show the test conditions.

Table 7
Condition Matrix for Out-of-Hatch

Condition Number	Seat Height SAE H30 (mm)	Gear Level
C01	LP	ENC
C12	LP	PPE
C13	LP + Offset	PPE
C14	LP - Offset	PPE
C15	LP	ACU

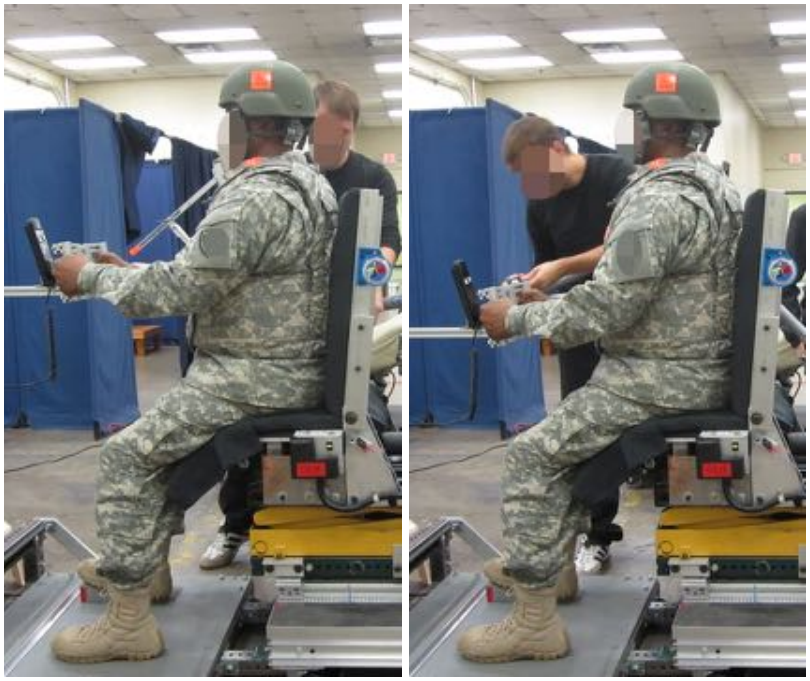

Figure 15. Out-of-hatch condition with two yoke positions: preference (left) and lowest possible when able to complete a quarter turn with both hands on the yoke.

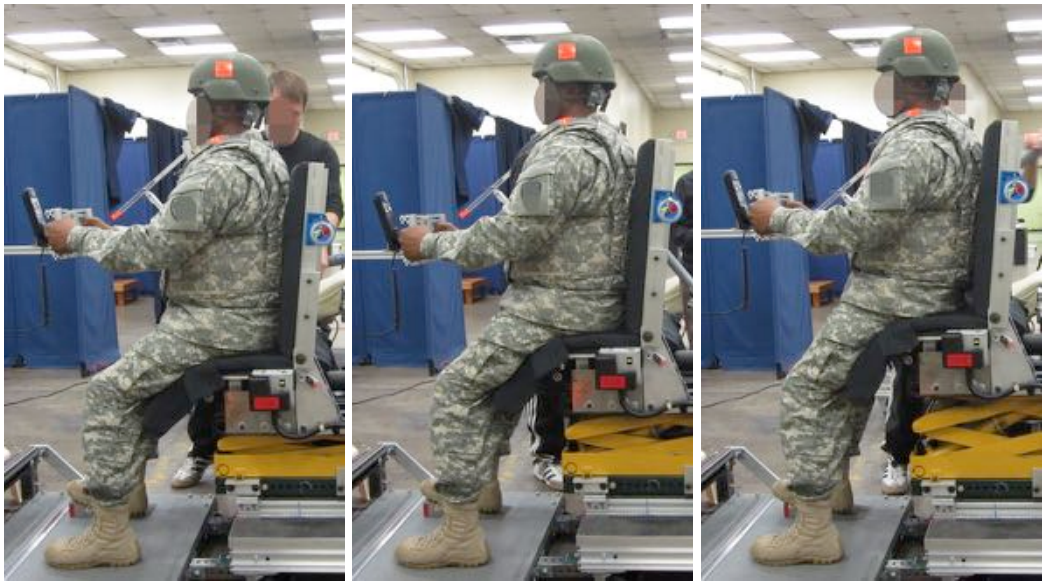

Figure 16. Out-of-hatch conditions at three different seat heights as a proportion of leg length from lowest to highest seat height (C14, C12, C1) from left to right.

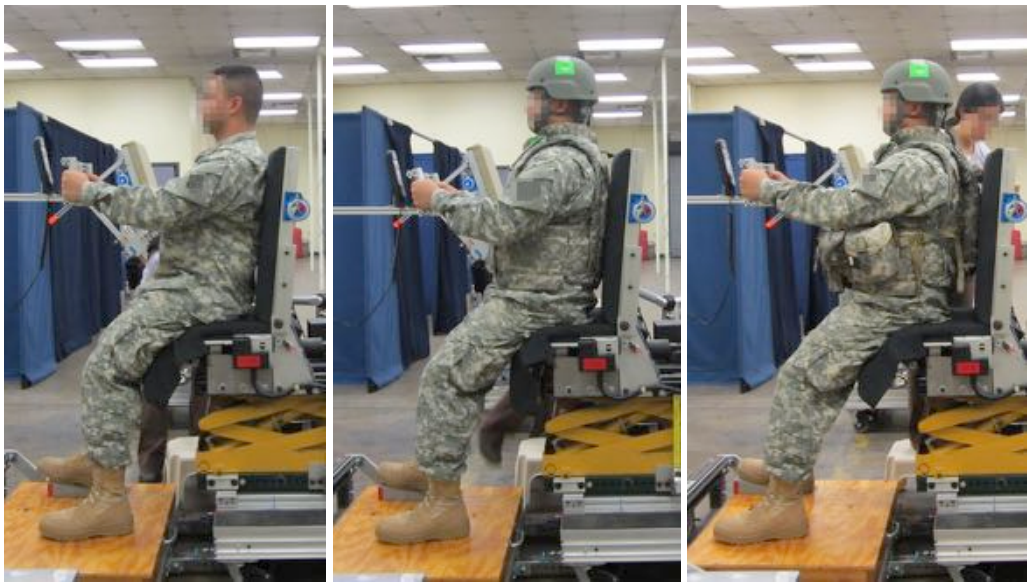

Figure 17. Out-of-hatch conditions with three levels of garb ACU(C15), PPE (C12) and ENC (C01) from left to right.

Highly Reclined Seating (HRS)

Figure 18 shows the mockup used for the highly reclined configurations. The HARP was established using the SAE J826 H-point was measured with the seat back at 30 degrees (Figure 19); this point was used as the HARP for all conditions. The aft part of the two-part seat pan was fixed in position and the angle of the forward part (under the thighs) was adjusted with the seat back angle. The height and fore-aft position of the foot plate could be adjusted manually. The upper portion of the seat back was fixed relative to the lower portion. These two sections pivoted as a unit around a location aft of the pan to provide back angle adjustment.

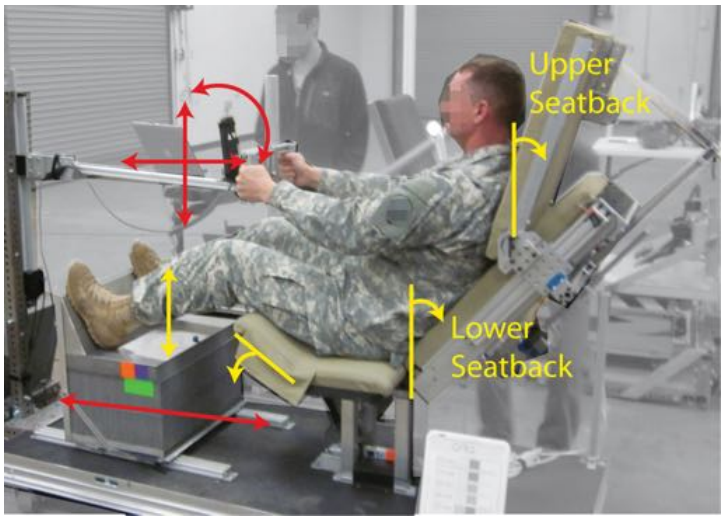

Figure 18. Highly reclined seat in which the Soldier positioned the foot platform fore-aft and the steering yoke up-down, fore-aft and tilt.

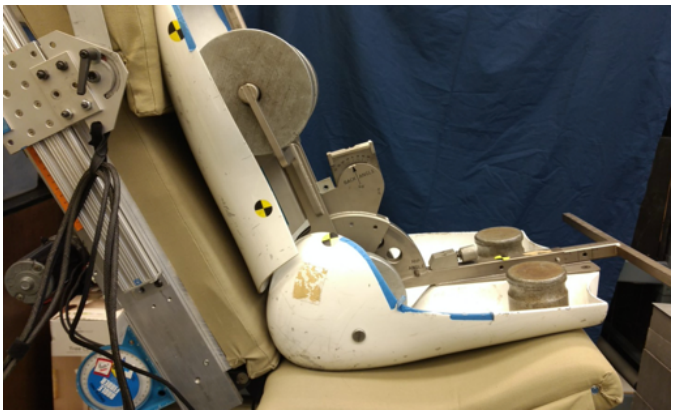

Figure 19. Measuring HARP location using the SAE J826 H-point machine in the HRS mockup.

Figures 20-22 and Table 8 show the test conditions. Testing was conducted at three seat back angles (angle of the lower portion of the seat back at 30, 40, and 50 degrees to vertical). At the middle seat back angle, data were gathered with three seat heights. All data were gathered at the PPE ensemble level, except that the condition with the middle seat back angle and highest seat height was repeated with ACU only.

Figure 20. Highly reclined seat at three levels of garb ACU (C18), PPE (C04), ENC (C03)

Figure 21. Highly reclined seat at three seat heights 100 mm (C05), 150 mm (C04) and 200 mm (C06)

Figure 22. Highly reclined seat at three back angles 30˚ (C08), 40˚ (C04), 50˚ (C07)

Table 8
Condition Matrix for Highly Reclined Seat

Condition Number	Seat Back Angle Re Vertical (deg.)	Seat Pan* Angle Re Horizontal (deg.)	Seat Height† (mm)	Gear Level
C03	40	35	150	ENC (no Camelbak)
C04	40	35	150	PPE
C05	40	35	100	PPE
C06	40	35	200	PPE
C07	50	40	150	PPE
C08	30	30	150	PPE
C18	40	35	200	ACU

* Front portion of pan under distal thighs.
† HARP above heel surface

Landmark Data

In each condition, the FARO Arm coordinate digitizer was used to record the three-dimensional location of the landmarks and reference points listed in Table 9.

Table 9
Landmarks and Reference Points Recorded in Mockups

C7 (Cervicale)	Most Forward Point on Torso
Back Of Head/Helmet Max Rearward	Most Lateral Point on Torso (Right)
Top Of Head/Helmet Max Height	Most Lateral Point on Thigh (Right)
Tragion (Right)	
Ectoorbitale (Right)	**On PPE and ENC**
Infraorbitale at Pupil Center (Right)	Helmet (3 Reference Points)
Glabella	IOTV (3 Reference Points)
Top of Hand Grip (Right)	TAP (3 Reference Points)
Ulnar Styloid Process (Right)	Camelbak (3 Reference Points)
Lateral Humeral Epicondyle (Right)	
Anterior-Superior Acromion (Right)	**On Equipment or Mockup**
Suprasternale (if reachable)	Faro Arm Cart (3 Reference Points)
Substernale (if reachable)	Mockup Platform (3 Reference Points)
ASIS (Right and Left)	Seat Cushion (2 Reference Points)
Estimate of Greater Trochanter (Right)	Seat Back (2 Reference Points)
Back of Pelvis Compressed (Right)	Pedal (2 Reference Points)
Lateral Femoral Epicondyle (Right)	Foot Platform Height Point
Suprapatella (Right and Left)	Yoke (Center, Top and Bottom)
Infrapatella (Right)	
Lateral Ball of Foot (Right)	**Condition Specific**
Lateral Malleolus (Right)	OOH: Yoke in lower position (center, top and bottom)
Heel (Bottom edge of sole at midline, Right)	HRS: Upper Seat Back (2 Reference Points)
Toe (Bottom edge of sole, longest shoe point, Right)	FEP: Fixed-Eye-Point Box (3 Reference Points)

Laboratory Hard Seat

Data were also gathered from each participant in the laboratory hard seat shown in Figure 23. This seat allows posterior landmarks on the spine and pelvis to be measured along with the anterior landmarks that are accessible in the mockup seat. In the hard seat, participants wore athletic shorts and no shirt to facilitate landmark identification and measurement. The landmarks measured in the hard seat (Table 10) include a subset of those measured in the mockup in addition to a set of posterior spine and pelvis landmarks.

Figure 23. Hard seat

Table 10
Landmarks and Reference Points Recorded in Hard Seat

Back Of Head (max rearward)	Acromion (Right and Left)
Top Of Head (Vertex)	Lateral Humeral Epicondylel (Left)
Tragion (Left)	Medial Humeral Epicondyle (Left)
Ectoorbitale (Left)	Ulnar Styloid Process (Left)
Infraorbitale at Pupil Center (Left)	Radial Sytloid Process (Left)
Glabella	Suprasternale
Menton	Substernale
Lateral Femoral Epicondyle (Right and Left)	C7 (Cervicale)
Medial Femoral Epicondyle (Right and Left)	T4
Suprapatella (Right and Left)	T8
Infrapatella (Right and Left)	T12
Medial Malleolus (Left)	L1
Ball of Foot Medial (Left)	L2
Toe, Longest Tibiale (Left)	L3
Ball of Foot Lateral (Left)	L4
Lateral Malleolus (Left)	L5
Heel (Left)	
ASIS (Right and Left)	Hard Seat Platform (3 Reference Points)
PSIS (Right and Left)	Faro Arm Cart (3 Reference Points)

Dependent Measures

The calculation of dependent measured followed the methods in Reed and Ebert (2013). In brief, the hard seat data were used to estimate joint center locations in the spine, pelvis, and extremities to create a subject-specific kinematic linkage. This information was used with the landmarks obtained in the mockup conditions to estimate joint center locations.

Statistical analyses were conducted using linear regression to estimate the location of important body landmarks and mockup components as a function of anthropometric and mockup variables. These methods followed those used in previous work (Reed and Ebert 2013). In particular, potential predictors were included if they were statistically significant with $p<0.01$ and their inclusion increased the adjusted R^2 value for the regression by at least 0.02 (i.e., the variable accounted for at least two percent of the variance in the dependent measure).

Anthropometric predictors were stature, the ratio of erect sitting height to stature (SH/S), and body mass index (BMI, kg/m^2, computed as body weight in kg divided by stature in meters squared). The natural log (ln) of BMI was used rather than BMI because the distribution of ln(BMI) is closer to a normal (Gaussian) distribution, which is valuable for population accommodation modeling.

RESULTS: POSTURE PREDICTION MODELS

Fixed Eye Point (FEP)

Prior to statistical modeling, all of the data were expressed relative to the eye location measured in the trial. Consequently, the results neglect any variability in eye location due to adjustment or posture differences.

Tables 11 and 12 list the regression models computed from the landmark and joint-center data. The full model is obtained by multiplying the coefficients by the predictors and summing together with the intercept. X positive rearward of the eye location, Z is positive above. To facilitate application to accommodation modeling, the fore-aft accelerator heel point location (AHPX) is predicted as a function of seat height above the heel surface. Because the seat (and hip) location relative to the eye location is independent of the vertical offset between the heel and eye (the variable manipulated in the test matrix), the test conditions were effectively varying seat height. When predicting posture for individual Soldiers, the HARPZ is first predicted followed by AHPX. For accommodation models, the input for predicting the distribution of AHPX is the mean seat height (see Accommodation Models section, below).

Fore-aft seat position relative to the eye point was significantly related to all three anthropometric predictors, although the R^2 value was small (11%). The vertical seat position was related to stature and torso length (expressed by SH/S), but the R^2 value was much higher (0.81). The hip location relative to seat HARP was not related to BMI, unlike in some previous studies. This may be due to the relatively small range of BMI in the subject pool. The R^2 values were less than 25% for both coordinates.

The coordinates of the subjects' preferred steering yoke positions were further forward and lower for taller subjects. On average, lower yoke positions were measured for subjects with longer torsos) and more-forward yoke positions were recorded for subjects with higher BMI, likely due to greater abdomen extension.

The fore-aft location of the accelerator heel point (AHPX) in the subject's preferred position was modeled as a function of the subject-selected seat height and stature. As expected, taller subjects placed their heels further forward; higher seat heights (also associated with smaller stature) resulted in the feet placed more rearward, closer to the eye point and seat HARP. However, the residual variance not accounted for by these predictors is high, with a root-mean-square error (residual standard deviation) of 61 mm.

As expected from the seat height findings, the vertical knee location was associated with seat height and stature. The fore-aft location was associated with stature alone, while the knees are further outboard relative to seat centerline with higher BMI. The angle of the side-view vector from hip to eye was computed as an overall measure of torso recline. As expected from the seat HARP findings, the R^2 value was low. The distance between hip and eye is dominated by stature and SH/S with the highest R^2 value of all of the models (0.83).

Table 11
Regression Models for Posture Prediction (PPE Condition) for FEP Conditions

Variable	Intercept (mm)	Stature (mm)	Ln(BMI) (nat. log kg/m^2)	SH/S	Seat Height*	EyeZ†	R^2_{adj}	RMSE
HARPX	484	-0.0890	67.7	-1054			0.11	38.7
HARPZ	526	-0.4015		-927			0.81	16.4
HipReHARPX	366	-0.0693		-511			0.09	21.3
HipReHARPZ	-302	0.0813		296			0.23	11.8
YokeCenterX	176	-0.1589	-87.2				0.14	53.0
YokeCenterZ	408	-0.2281		-642			0.17	41.4
AHPX	36	-0.4447			0.259		0.33	61.3
AHPX	-7	-0.5520				0.315	0.36	60.0
Leg Angle**	24.6				0.081		0.21	7.6
Leg Angle**	1.1					0.0544	0.14	7.9
Thigh Angle**	47.3				-0.091		0.49	4.6
Thigh Angle**	51.9					-0.041	0.15	5.9
Hip-Eye Angle (deg)	-47			94.3			0.08	4.07
Hip-Eye Distance	-516	0.4022		930			0.83	15.3
Seat Back Angle (deg)	-33.7	0.0089		73.8			0.06	3.6

* Seat height calculated as HARPZ-AHPZ
† Eye height relative to heel surface height; use as an alternative to seat height in prediction of AHP and knee position. Note this value has **positive** values (typically between 900 and 1250 mm).
** Segment angles with respect to horizontal.

Table 12
Regression Models for Knee and Elbow Location for FEP Conditions

Variable	Intercept (mm)	Stature (mm)	Ln(BMI) (nat. log kg/m^2)	SH/S	Seat Height*	EyeZ†	R^2_{adj}	RMSE
SuprapatellaX re HARP	8	-0.2731					0.46	27.2
SuprapatellaY re HARP	500	-0.169	-124				0.44	29.5
SuprapatellaZ re HARP	-178	0.3106			-0.627		0.61	38.1
SuprapatellaZ re HARP	-184	0.5046				-0.555	0.54	41.7
SuprapatellaZ re AHPZ	-179	0.3127			0.368		0.48	38.2
SuprapatellaZ re AHPZ	-197	0.1859				0.366	0.49	37.8
ElbowX re HARP	318		-125				0.10	51.4
ElbowY re HARP	-101	0.0654	77.0				0.37	17.7
ElbowZ re HARP	-491		126	572			0.18	38.5

Table 13 shows the valid ranges of predictors based on the test conditions. Note that the models are configured so that EyeZ is the primary predictor, but limits on seat height are shown as well. High eye points above the floor (AHP) may require seat heights for small drivers that are too high for them to comfortably reach the floor. Generally, seat heights above about 435 mm begin to cause disaccommodation for small women.

Table 13
Valid Range of Predictors for FEP Models (mm)

Predictor	Low Limit	High Limit	Acceptable Extrapolation	Cautions
Seat Height (HARP above AHP)	300	550	±50	Seat heights above about 435 mm will create disaccommodation for small drivers that is not represented in the accommodation models
EyeZ (eye point above AHP)	900	1250	±50	High eye points may result in disaccommodation based on seat height for small drivers that is not represented in the accommodation models

Table 14 shows the effects of the ensemble relative to the PPE condition represented by the equations in Tables 11 and 12. The largest effects were observed on the seat position. Soldiers wearing body armor and gear placed the seat further rearward, although the effect on the hip location with respect to seat HARP was minimal. Seat back angles were more reclined with body armor and gear, though the torso was more upright (a total of 7 degrees more upright in ACU than in ENC). Table 15 lists regression equations for body segment angles. These are useful for posturing manikins or other kinematic representations of drivers.

Table 14
Ensemble Effects Relative to PPE Condition for FEP Conditions

Variable	ACU	BBG (ENC)
HARPX	-51	70
HARPZ	8	-7
HipReHARPX	10	--
HipReHARPZ	--	--
YokeCenterX	--	--
YokeCenterZ	--	--
AHPX	-14	41
SuprapatellaX re HARP	-10	--
SuprapatellaZ re HARP	--	--
ElbowX re HARP	54	-72
ElbowY re HARP	-20	10
ElbowZ re HARP	-14	28
Hip-Eye Angle (deg)	3	-4
Hip-Eye Distance	--	--
Seat Back Angle (deg)	-1.0	1.9

Table 15
Regression Models Predicting Body Segment Angles for FEP Conditions

Angle	Intercept (mm)	Stature (mm)	ln(BMI) (nat. log kg/m^2)	H30	Hip-Eye Angle (deg)	R^2_{adj}	RMSE
Head	-15.9	0.0129				0.03	6.5
Tragion*	-42.9	0.0129				0.03	6.5
Neck	-2.7						
Thorax	-41.2	0.0092	5.55		1.27	0.74	3.8
Abdomen	58.2	-0.0091	-6.68		1.33	0.54	6.2
Pelvis	78.2		-10.1		0.528	0.08	10.3
Thigh wrt Horiz	1.8	0.0265		-0.091		0.64	3.8
Knee	184	-0.0405			-0.881	0.26	10.2
Leg wrt Vertical	24.6			0.081		0.21	7.6

* Angle of vector from head-neck joint to tragion wrt vertical (positive rearward).

Out of Hatch (OOH)

Tables 16 and 17 list posture-prediction models for the OOH condition. For maximum flexibility in application, key landmark locations are expressed relative to AHP, HARP, and eye. Moreover, separate regression models are presented for some variables using both seat height and AHPZ (vertical distance from eye to heel surface) as alternative predictors. Torso posture was not substantially affected by the seat height conditions. The torso was slightly more reclined at higher seat heights (contrary to expectation), but the effect was small. Table 18 shows clothing/gear ensemble effects on key variables (effects on variables not listed were negligible). The offsets are expressed relative to the PPE condition.

The steering yoke was measured in two positions. Table 19 lists regression predictions for yoke location (center point of yoke) for the Soldiers' preferred position. Table 20 lists predictions for the "lowest possible" position where they could still execute a quarter turn with both hands on the yoke.

Table 21 lists regression equations for body segment orientations. These are useful for manikin posture prediction or depicting the body as a kinematic linkage. The thigh and leg angle predictions are also used with the knee contours to create clearance planes.

Table 16
Regression Models for Posture Prediction (PPE Condition) for OOH Conditions

Variable	Intercept (mm)	Stature (mm)	Ln(BMI) (nat. log kg/m^2)	SH/S	Seat Height*	EyeZ†	R^2_{adj}	RMSE
HipReHARPX	490	0.2757	-63.6	-638	-0.601		0.68	20.9
HipReHARPZ	-263	0.1321	24.8		-0.087		0.27	16.2
HARPReEyeX	-297		80.3		0.28		0.25	36.6
HARPReEyeX	-310		82.8			0.132	0.17	38.5
HARPReEyeZ	487	-0.5837		-743	0.294		0.83	15.5
HARPReEyeZ	713	-0.6093		-1129		0.173	0.72	20.0
HARPReAHPX	376							44.8
HARPReAHPZ	714	-0.5756		-1137		1.137	0.91	20.3
AHPReEyeX	-225							67.4
Hip-Eye Angle (deg)	-91.3			130	0.019		0.16	3.3
Hip-Eye Angle (deg)	-79.3			109		0.010	0.11	3.4
Hip-Eye Distance	-325	0.4771		729	-0.251		0.77	16.0
Hip-Eye Distance	-518	0.3672		1079			0.64	20.0

* Seat height calculated as HARPZ-AHPZ
† Eye height relative to heel surface height relative; use as an alternative to seat height in prediction of AHP and knee position. Note this value has **positive** values.

Table 17
Regression Models for Knee and Elbow Locations (PPE Condition) for OOH Conditions

Variable	Intercept (mm)	Stature (mm)	Ln(BMI) (nat. log kg/m^2)	SH/S	Seat Height*	AHPZ†	R^2_{adj}	RMSE
SuprapatellaX re HARP	-95	-0.1548			-0.114		0.43	21.1
SuprapatellaY re Centerline	-481	0.2116	138		-0.239		0.39	30.1
SuprapatellaY re Centerline	-489	0.4432	140			0.405	0.47	28.3
SuprapatellaZ re HARP	-70	0.3631			-0.960		0.92	15.11
SuprapatellaZ re HARP	-19	0.7882				1.07	0.69	29.4
SuprapatellaX re AHP	-72							51.4
SuprapatellaZ re AHP	323	0.3235			-591		0.75	17.7
SuprapatellaX re Eye	-297							40.7
SuprapatellaZ Eye	795	-0.2446		-1321	-0.711		0.88	20.5
SuprapatellaZ Eye	313	0.2463		-562		0.912	0.91	17.4
ElbowReHARPX	-208							57.4
ElbowReHARPY	-97		108				0.29	23.8
ElbowReHARPZ	221							49.4

Table 18
Effects of Clothing/Gear Ensemble on Posture Variables relative to PPE Condition for OOH Conditions

Variable	ACUrePPE	ENCrePPE
HARPReEyeX	-39	79
HARPReEyeZ	3	-9
HARPReAHPX	-16	9
HARPReAHPZ	0	3
HipReHARPX	18	-30
HipReHARPZ	0	31
HipReEyeX	-27	37
HipReEyeZ	6	-34
YokeReHARPX*	24	-85
YokeReHARPZ	-23	69
YokeReEyeX	-15	-6
YokeReEyeZ	-20	60
YokeReAHPX	8	-76
YokeReAHPZ	-23	72
AHPReEyeX	-23	70
SuprapatellaX re HARP	12	-20
SuprapatellaZ re HARP	--	--
SuprapatellaX re EyeX	-27	60
SuprapatellaZ re EyeZ	--	--
SuprapatellaX re AHPX	--	--
SuprapatellaZ re AHPZ	--	--
Hip-Eye Angle (deg)	2.2	-2.7
Hip-Eye Distance	-9	38
ElbowReHARPX	35	-98
ElbowReHARPY	-15	7
ElbowReHARPZ	-3	49

* Use the same values for low-yoke position (Table 20)

Table 19
Regression Models for Preferred Yoke Position for OOH Conditions

Variable	Intercept (mm)	Stature (mm)	Ln(BMI) (nat. log kg/m^2)	SH/S	Seat Height*	AHPZ†	R^2_{adj}	RMSE
YokeReHARPX	95.4		-118		-0.259		0.13	64.8
YokeReHARPX	123		-119			0.159	0.10	65.8
YokeReHARPZ	321							72.1
YokeReEyeX	-342.4							68.7
YokeReEyeZ	-342.2							73.5
YokeReAHPX	-117							78.6
YokeReAHPZ	49.2	0.6134					0.27	79.9
YokeReAHPZ	169	0.2257			0.687		0.41	72.1
YokeReAHPZ	413				0.866		0.39	73.1
YokeReAHPZ	24.3					-0.745	0.43	70.7
YokeReAHPZ	156	-0.2800				-0.985	0.44	70.2

Table 20
Additional Regression Models for Low Yoke Position for OOH Conditions

Variable	Intercept (mm)	Stature (mm)	Ln(BMI) (nat. log kg/m^2)	SH/S	Seat Height*	AHPZ†	R^2_{adj}	RMSE
YokeReHARPX (low)	121		-119		-0.286		0.15	63.5
YokeReHARPX (low)	147		-120			0.172	0.11	64.9
YokeReHARPZ (low)	226							76.1
YokeReEyeX (low)	-340							66.8
YokeReEyeZ (low)	-438							81.5
YokeReAHPX (low)	-115							81.5
YokeReAHPZ (low)	139	0.5040					0.18	85.3
YokeReAHPZ (low)	412				0.866		0.39	73.1
YokeReAHPZ (low)	46					-0.663	0.33	76.8

Table 21
Regression Models Predicting Body Segment Angles for OOH Conditions

Angle	Intercept (mm)	Stature (mm)	ln(BMI) (nat. log kg/m^2)	SH/S	AHPZ re Eye	ACU/ ENC	R^2_{adj}	RMSE
Head	0.6							7.7
Tragion*	-26.4							7.7
Neck	-8.7							7.8
Thorax	-130	0.0231		141		1.1/-2.1	0.11	5.0
Abdomen	97.3	-0.0869	-13.9		-0.073	3.3/-7.1	0.32	5.7
Pelvis	14.7	-0.1293			-0.166	6.7/0	0.07	10.1
Thigh	-39.0	0.1272			0.147		0.62	4.5
Leg	0.4							1.2

* Angle of vector from head-neck joint to tragion wrt vertical (positive rearward).

These predictions are valid over the experimental range as well as some reasonable extrapolation. Table 22 shows the recommended range of input variables. In the experiment, the vertical offset between the floor and eye was varied based on stature. Figure 24 shows the distribution of floor-eye vertical offsets for the OOH conditions. By design, each subject's highest condition was approximately the highest for which they could sit on the seat; higher eye locations would require them to stand, perhaps leaning against the seat. The figure illustrates the design challenge for an OOH condition in which each driver's eye location should be about the same. If the floor is more than about 1350 mm below this eye location, the shortest drivers will not be able to sit at all.

An absolute boundary can be calculated from the shortest driver eye heights. In ANSUR II, the mean difference in height of the eye and vertex (top of the head) is about 110 mm, so we can estimate the eye height in the vehicle for a standing person by subtracting 110 mm from stature and adding 35 mm for boot thickness, or subtracting a net 75 mm. Using the 5th-percentile female stature in ANSUR II of 1525 mm, the maximum height above the floor for a driver eye point accessible to 95% of Army women is 1450 mm. Referring to Figure 24, this is about the midpoint of the distribution of test conditions, recalling that these are all *seated* test conditions. So, a floor-to-eye vertical offset of not more than 1300 mm would allow nearly all drivers to sit, while a 1450 mm offset would allow nearly all Soldiers to drive, though the shorter ones would be forced to stand.

The design solutions will depend on the constraints of the particular vehicle, including the adjustment ranges available for the seat and steering controller. For a particular design, the posture prediction models presented above can be used to estimate postures for people with a wide range of body size. In general, the models will be valid when the distance from floor to eye is within the range in Figure 24 for the stature of interest. Quantitatively, the models are valid when the floor-to-eye distance is at least 250 mm less than stature. For conditions in which the floor-to-eye distance is larger, the lower-extremity postures can be expected to differ, with drivers tending to stand rather than sit.

Table 22
Valid Range of Predictors for OOH Models (mm)

Predictor	Low Limit	High Limit	Acceptable Extrapolation	Cautions
Seat Height (HARP above AHP)	650	950	±50	These ranges assume that the seat permits downward sloped thigh angles without restriction.
EyeZ (eye point above AHP)	1250	1650	±50	High eye points may result in disaccommodation for the shortest drivers (see text).

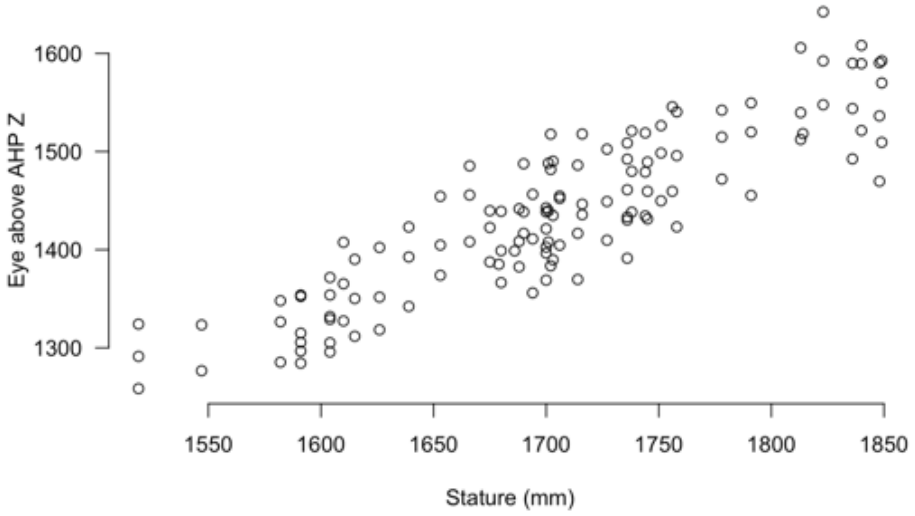

Figure 24. Eye locations above the heel surface (AHP) in OOH conditions.

Highly Reclined Seating (HRS)

Table 23 shows regression models for the HRS conditions. All landmark locations are expressed relative to the seat HARP, which remained fixed in position for all trials. As expected, the seat back angle had strong effects on torso posture variables. Unexpectedly, the seat height did not significantly affect the fore-aft heel location, possibly due to the relatively small range of seat heights used.

Body segment orientations are predicted two ways. Table 24 lists predictions based on the anthropometric variables as well as seat back angle and seat height, while Table 25 lists predictions based on hip-eye angle only. The latter models are useful for obtaining kinematically consistent predictions when hip and eye locations are predicted separately.

Table 26 lists the effects of gear/clothing ensemble on posture variables. Offsets for ACU and ENC are presented relative to the PPE condition. Surprisingly, higher levels of gear did not change hip location with respect to HARP. This finding is likely due to the fairly flexed pelvis/lumbar postures in the seat, such that space was available behind the pelvis even in the ACU condition. Ensemble strongly affected torso recline measures, such as hip to eye, with the gear pushing the torso more upright at each fixed seat back angle.

Table 23
Regression Equations for HRS Conditions

Variable*	Intercept	Stature	SH/S	ln(BMI)	BA**	H30	R^2_{adj}	RMSE
HipX	-14.5							26.9
HipZ	-5							
EyeX	-184				7.70		0.81	30.5
EyeY								15.9
EyeZ	-480	0.393	621	63.5	-2.85		0.81	20.3
Hip-Eye Angle	12.7			-8.76	0.714		0.68	4.1
Hip-Eye Distance	-540	0.403	740	41.8	-0.936		0.84	15.1
AHPX	-995	-0.250	1093				0.23	54.2
SuprapatX	-192	-0.126				-0.238	0.21	27.2
SuprapatY	-514	0.181		117			0.24	43.5
SuprapatZ	-82	0.319		-69.1		-0.346	0.33	42.6
YokeX	45			-157	6.02		0.46	59
YokeZ	413							46.5
ElbowX	38.7			-82.2	5.07		0.63	33.7
ElbowY	-178	0.114		72.5			0.41	18.6
ElbowZ	-290			162			0.23	41.0
ShoulderJntX	121			-54.0	6.11		0.84	22.2
ShoulderJntY	-52.5	0.081		25.4			0.22	15.7
ShoulderJntZ	-122	0.253		51.7	-2.64		0.67	23.1
AnklereAHPX	81							
AnklereAHPZ	107							

* mm and deg wrt HARP (SIP).
** Seat back angle wrt vertical (range 30 to 50 deg).

Table 24
Regression Equations for Body Segment Orientations for HRS Conditions

Variable	Intercept	Stature	SH/S	ln(BMI)	BA	H30	R^2_{adj}	RMSE
PelvisAngle	98.5			-16.8	0.455		0.16	9.9
LumbarAngle	70.5			-20.3	0.773		0.57	6.1
ThoraxAngle	-26.9				0.910		0.57	6.4
NeckAngle	-7.7				0.151		0.06	4.8
HNTragAngle	-32				0.275		0.12	5.9
HeadAngle	-4.9				0.275		0.12	5.9
ThighAngle re Horiz	4.9	0.032		-9.50		-0.043	0.20	6.3
Hip-C7 Angle	-31.4			9.64		-0.796	0.68	4.6
LegAngle re Vertical	69.2	-0.022		13.4		-0.103	0.35	6.7

Table 25
Body Segment Orientations as a Function of Hip-Eye Angle for HRS Conditions

Variable	**Intercept**	**HipEye**	**R^2_{adj}**	**RMSE**
PelvisAngle	52.8	0.746	0.25	9.3
LumbarAngle	21.9	1.07	0.70	5.1
ThoraxAngle	-7.4	1.33	0.86	3.7
NeckAngle	-5.1	0.262	0.15	4.5
HNTragAngle	-24.1	0.252	0.08	6.1
HeadAngle	2.9	0.252	0.08	6.1

Table 26
Ensemble Effects relative to PPE Condition for HRS Conditions

Variable	ACU	ENC
HipX	--	--
HipZ	--	--
EyeX	52	-13
EyeZ	-35	4
Hip-Eye Angle	4.9	-1.7
Hip-Eye Distance	-22	0
YokeX	47	-21
YokeZ	-47	19
ElbowX	57	-19
ElbowY	-14	13
ElbowZ	-40	34
ShoulderJntX	43	-6
ShoulderJntY	--	--
ShoulderJntZ	-35	5

Table 27 shows the valid ranges of input variables, which cover the experimental range as well as some reasonable extrapolation. For seat height, the experimental range was 100 to 200 mm. The findings are probably valid for seat heights from 50 to 250 mm. The results will be expected to be valid for the experimental seat back angle range of 30 to 50 degrees. The findings are probably valid for fixed back angles from 25 to 55 degrees.

Table 27
Valid Range of Predictors for HRS Models (mm and deg)

Predictor	Low Limit	High Limit	Acceptable Extrapolation	Cautions
Seat Height (HARP above AHP) (mm)	100	200	±50	Higher and lower seat heights assume that the front of the seat cushion is angled appropriately to avoid interference while supporting the thighs.
Seat Back Angle (deg)	30	50	±5 deg	More-upright seat back angles may not be feasible with very low seat heights; more-reclined seat back angles would be expected to require head support

RESULTS: POPULATION ACCOMMODATION MODELS

Overview

The development of population accommodation models followed the general procedures presented in Zerehsaz et al. (2014a, b) for the fixed-heel driver and squad seating. The regression models presented above are used to predict mean responses for male and female sub-populations. The variance in the response (for example, eye location in HRS) is predicted by considering both anthropometric variation and the residual variation in the response that is not accounted for by the vehicle, seat, or anthropometric variables. This residual is represented by the root mean square error (RMSE) in the regression tables. Appendix B provides general background on the formulation of accommodation models.

Different accommodation models were developed for each driver condition, depending on the constraints and variables in the test setup. Table 28 lists the models for each mockup condition.

Microsoft Excel workbooks have been created that embody these accommodation models. The Excel workbooks are considered to be the authoritative implementation of the accommodation models. If discrepancies are found between the Excel workbooks and this report, the Excel workbooks should take precedence. This report documents the procedures and differences among the models across seating configurations. For the examples, target accommodation was 90%.

Table 28
Accommodation Model Availability by Configuration

	FEP	OOH	HRS
Eyellipse			X
Helmet Contour	X	X	X
Seat Adjustment	X	X	
Steering Position	X	X	X
Steering Position (Low)		X	
Pedal Fore-aft Adjustment	X	X	X
Back Angle Adjustment	X		
Knee Clearance	X	X	X
Elbow Clearance	X	X	X
Elbow Clearance (non-driver)	X		

Anthropometry Inputs

The anthropometry inputs are the same as in the previous model development work. Table 29 lists the inputs, which are the means and standard deviations of four variables for men and women. The values in Table 29 were obtained from ANSUR II, but values for any other population can be used as appropriate. In addition to these variables, the fraction of the population that is male is used in all calculations. In the examples in the sections that follow, the reference population is ANSUR II with 90% male.

Table 29
Reference Anthropometric Inputs from ANSUR II

Dimension	**Men**		**Women**	
	Mean	SD	Mean	SD
Stature (S), mm	1756	68.6	1628	64.2
Erect Sitting Height (SH), mm	918	35.7	857	33.1
Erect Sitting Height / Stature (SHS)	0.523	0.0135	0.526	0.0141
Log(BMI)*, log(kg/m^2)	3.31	0.146	3.23	0.135

* Natural log; in Excel, use ln()

Calibration and Ensemble Inputs

The clothing/gear ensemble is entered as ACU, PPE, or ENC (BBG). As noted above, the default for the regression and accommodation models is PPE, with the other conditions applied as offsets. Generally, ensemble affects the hip location on the seat, and hence seat fore-aft position, along with steering and elbow locations. For HRS, ensemble has a strong effect on measures of torso posture (e.g., eye location). Note that if a seat has relief for the hydration pack, ENC is taken as equivalent to PPE.

The HARP can be established using either the SAE J826 H-point machine or the Seat Index Point Tool (SIPT). Choosing the SIPT shifts the estimated location of the HARP with respect to the seat by 5 mm; this effect is added into calculations related to fore-aft HARP location.

Table 30
Inputs for FEP Accommodation Models

Variable	Definition
Calibration Tool	SAE J826 H-point machine or Seat Index Point Tool. The SIP is assumed to lie 5 mm rearward of H-point. Either point is termed the Human Accommodation Reference Point (HARP) in the models.
Ensemble	ACU, PPE, or BBG (ENC)
Hydration Relief	Whether the seat has a cut-out for the hydration pack; if so, the ensemble level is considered to be PPE for purposes of hip location with respect to the seat

Accommodation Models for Driver with Fixed Eye Point (FEP)

Inputs

In addition to variables listed above, the eye height above the floor is the primary input to the FEP models. The origin is taken as a point on the floor (heel rest) plane at the fore-aft location of the eye point. For the illustrations below, the value was taken as 1100 mm (midpoint of experimental range).

Outputs

Figure 25 illustrations the contours generated by the accommodation models in side-view.

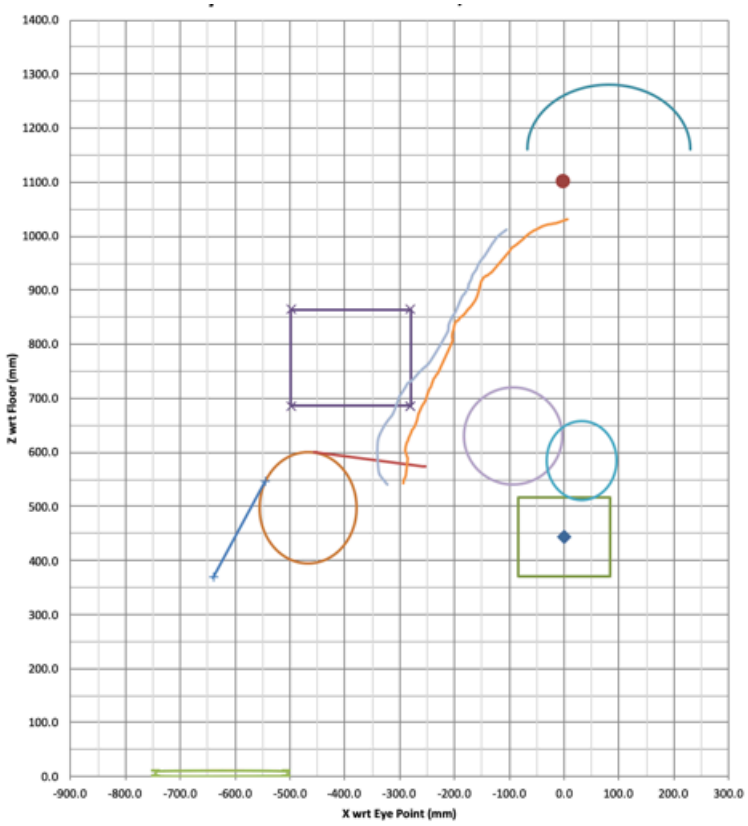

Figure 25. Side-view illustration of contours generated by FEP accommodation models.

Seat Adjustment Range

The vertical and horizontal seat adjustment range were calculated jointly such that the total accommodation is 90%. For FEP, the adjustment range is computed relative to the eye point in X (fore-aft) and with respect to the floor in Z (vertical). Note that the fore-aft position and length are not affected by the eye height above the floor. The fore-aft adjustment range of 167 mm is approximately centered below the eye point.

The vertical position of the seat adjustment range is determined predominantly by anthropometric variables, so that the seat adjustment range effectively lies a fixed distance below the eye point. Changing the fraction of men in the population has the largest effect on this offset.

Note that because the vertical seat adjustment range prediction is tied to the eye point, high eye points relative to the floor can result in disaccommodation for short-statured drivers. Because these drivers also tend to have short torsos, they will need seat positions near the top of the adjustment range to be able to attain the needed eye location. Although the extent of disaccommodation depends on such things as the seat cushion length and angle, a rough measure of the desirable upper bound can be obtained from consideration of the lower quantiles of popliteal height for women. In the female data from ANSUR II, the 5th-percentile seated height of the back of the knee with the leg vertical (popliteal height) is 350 mm. Adding 35 mm for boots, and considering that the H-point could lie approximately 50 mm above the front edge of the cushion, the upper edge of the seat adjustment range should ideally be no more than 435 mm above the floor. However, a higher limit value might be appropriate for a population that is more than 50% male.

Torso Contour

The torso contour represents a side-view and top-view contour for the PPE and ENC conditions. For FEP, the contours were positioned relative to the middle of the seat position adjustment range based on the contour calculations used for the fixed-heel model (Zerehsaz et al. 2014b). To account for the more-upright torso posture, the contours were rotated more upright around the mean HARP position by the difference between the predicted mean hip-eye angle (see Table 11) and the value obtained in the fixed-heel study (assumed constant at 1 degree aft of vertical). Table 31 lists the locating equations relative to mean seat position, adapted from the previous work. Note that the correlation with seat position is included in the calculations of the fore-aft variance. Figure 26 illustrates the torso contour outputs. The points defining the torso contours relative to the reference points are listed in Appendix C.

Table 31*
Locating Equations Relative to Mean HARP for Torso Contour Reference Points

Reference Point	Constant	Stature	Ln(BMI)	SH/S	R^2_{adj}	RMSE	Correlation with Seat Position
PPE-X	-215		92.9		0.23	25.1	-0.18
PPE-Z	-408	0.156	119	349	0.71	13.3	
ENC-X	188.8	-0.095	75.2		0.13	31.7	-0.4
ENC-Z	299						

* Adapted from Table 7 in Zerehsaz et al. (2014b)

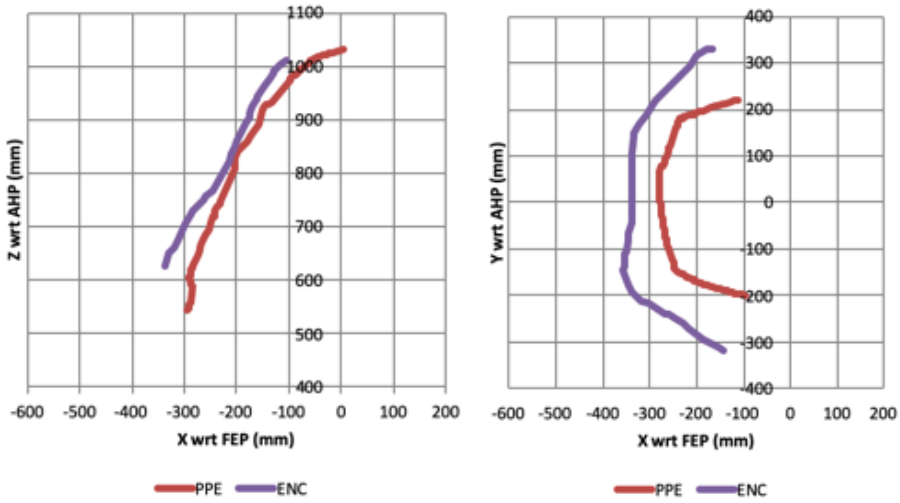

Figure 26. Torso contours in sideview (left) and top view (right).

Steering Yoke Position

In each test condition, the participant selected their preferred vertical and fore-aft position for the steering yoke. The distribution of the center point between the handles is modeled in this report. The calculations are very similar to those for seat position. The location relative to the eye point and floor is independent of the eye height above the floor but is influenced by anthropometry and ensemble level (see posture prediction equations, above). Fore-aft and vertical location are modeled independently because no correlation was noted between these variables.

Pedal Position

The participants in the FEP trials first adjusted the seat, then adjusted the fore-aft position of the pedal assembly to a comfortable position. The location of the accelerator heel point (AHP) was recorded. For purposes of accommodation modeling, the mean vertical seat position is taken as an input, along with mean stature. The calculations using eye height above floor as the input would be approximately equivalent. For the reference population and 90% accommodation, the range of pedal adjustment required is 237 mm, with a center point located 624 mm forward of the eye point.

Helmet Contour

In prior work (Reed and Ebert 2013), the average front- and side-view profiles of the advanced combat helmet (ACH) relative to the eye and head centerline were documented (see Appendix D). Due to different helmet sizes and positioning, the standard deviation of the top of the helmet height (Z coordinate) with respect to the eye was 10.9 mm. This was used with the standard normal distribution assumption and the mean helmet height of 161.8 mm to compute the cutoff contour for the target accommodation level. Similarly, the front and rear cutoffs were established using the corresponding standard deviation in the data of 8.5 mm. The lateral margin of the cutoff used the mean value, i.e., no lateral

variance was modeled. However, a 23-mm head turn allowance derived from SAE J1052 was added to both sides of the contour.

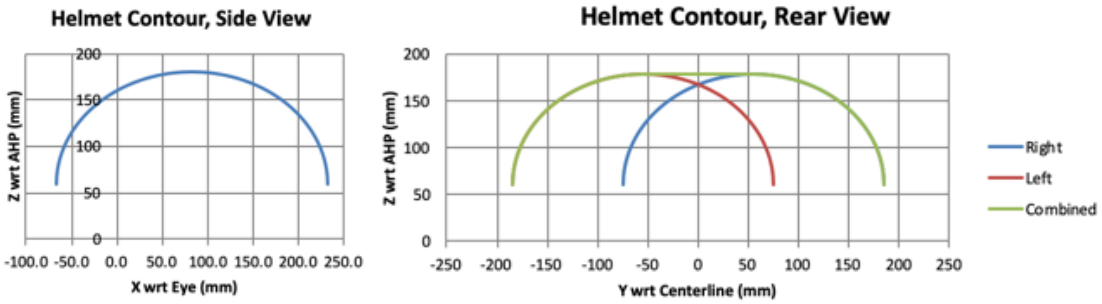

Figure 27. Helmet cutoff contours for 95% accommodation.

Knee Contour

Knee clearance contours are based on modeling of the location of the suprapatellar landmark with respect to the eye (X), seat centerline (Y), and HARP (Z). The mean vertical location of the HARP is added to express the result relative to the floor.

Using the same methods applied for other landmarks, a 3D cutoff ellipse is computed for the suprapatellar landmark. The leg segment angle with respect to vertical and the thigh segment angle with respect to horizontal are computed from the corresponding regression equations. A tibia landmark location is computed by rotating a standardized offset relative to suprapatellar of {-22, -47} mm by the leg angle. The X and Z axes of the contour are extended downward and forward to accommodate the tibia landmark and a new centroid is computed. A standard knee width of 110 mm is used to extend the ellipse laterally. Finally, tangents to the ellipse at the tibia and thigh segment angles are constructed in side-view to represent the front of the leg and top of the thigh.

Elbow Contour

Elbow clearance contours were created based on modeling the lateral humeral epicondyle landmark location, with adjustments for the olecranon process. Elbow location was modeled with respect to the eye point (X & Z) and seat centerline (Y). The elbow contour relative to the eye is affected by anthropometry and ensemble level but not by the seat or eye point height. Using the same process as for other contours, the centroid is computed from the mean anthropometry values for men and women and adjusted for ensemble level (Y and Z only). The vertical axis length was extended downward by 35 mm to accommodate the olecranon process. The eye location with respect to the floor (AHPZ) was subtracted to express the contours with respect to eye (X), centerline (Y), and floor (Z) for consistency with the other models.

Accommodation Models for Out-of-Hatch Driver

Inputs

In addition to variables listed above for all models, the eye height above the floor is the primary input to the FEP models. The origin is taken as a point on the floor (heel rest) plane at the fore-aft location of the eye point. For the illustrations below, the value was taken as 1450 mm (midpoint of experimental range).

Outputs

Figure 28 illustrates the contours generated by the accommodation models in side view.

Seat Adjustment Range

The vertical and horizontal seat adjustment range were calculated jointly such that the total accommodation is 90%. For OOH, the adjustment range is computed relative to the eye point in X (fore-aft) and with respect to the floor in Z (vertical). Note that the fore-aft position and length are not affected by the eye height above the floor. The fore-aft adjustment range of 157 mm is located rearward of the eye point. As with the FEP accommodation models, the relatively large (173-mm) vertical adjustment range is needed to accommodate the range of torso lengths with a fixed eye point.

The vertical position of the seat adjustment range is determined predominantly by anthropometric variables, so that the seat adjustment range effectively lies a fixed distance below the eye point. Changing the fraction of men in the population has the largest effect on this offset.

High eye points result in concerns about disaccommodating short drivers that are similar to those with FEP. However, the seat used in an OOH configuration is assumed to allow downward-angled thighs without restriction, so much higher seats are feasible.

Torso Contour

Torso contours were constructed in the same manner as with FEP, using the mean HARP location as the reference. As with FEP, the torso contours were rotated relative to the original FHP model results using the hip-to-eye angle. Typically, the contours are 10 degrees more upright than for FHP.

Steering Yoke Position

In each test condition, the participant selected their preferred vertical and fore-aft position for the steering yoke. This distribution was computed in the same manner as for FEP. In addition, the partipants demonstrated the lowest yoke position at which they could rotate the yoke at least 90 degrees in both directions. A model of this location was also developed. The adjustment range is similar in size and located about 100 mm lower than the preferred range.

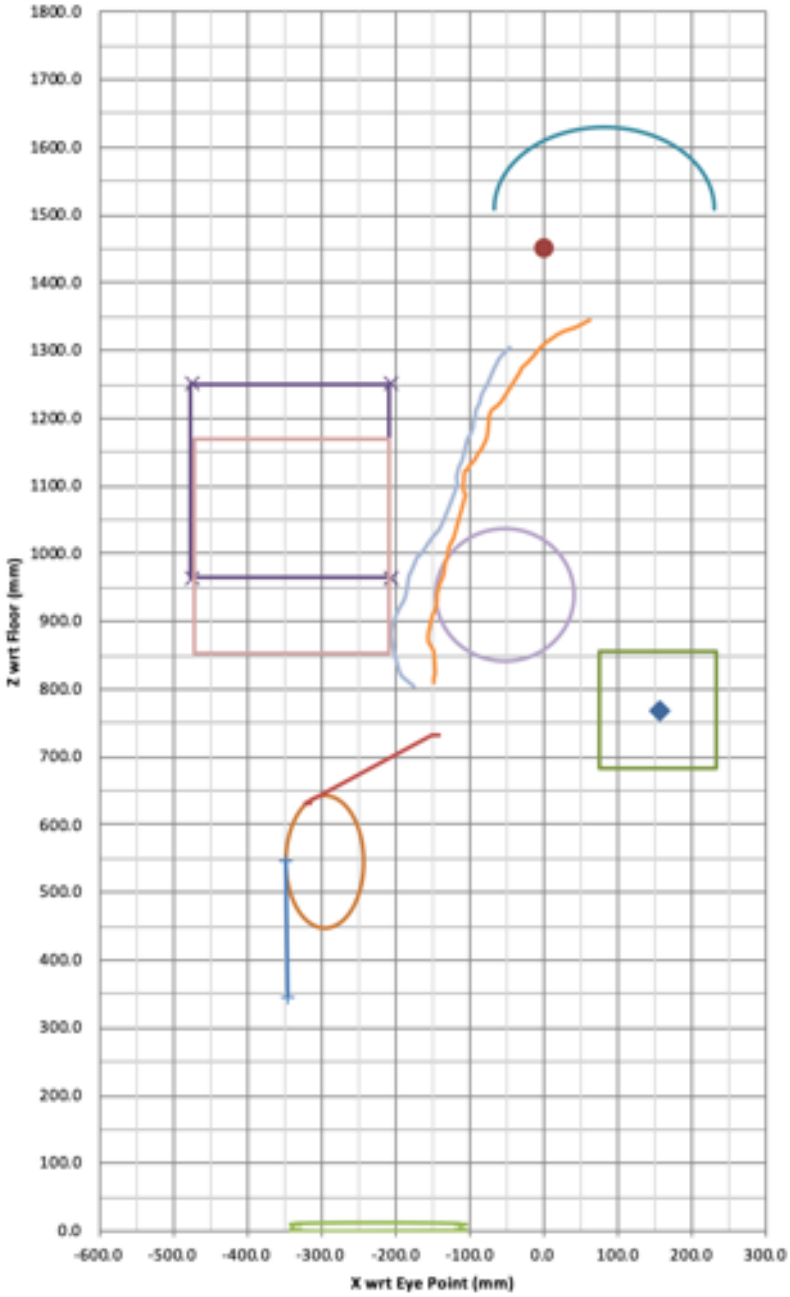

Figure 28. Side-view illustration of OOH accommodation contours.

Pedal Position

The preferred pedal position was estimated by placing a thin wedge under the participant's right foot in a comfortable location. Pedal position was unaffected by any

subject or configuration variables, and so the distribution is modeled from the observed standard deviation. Note that due to the posture a single pedal position might accommodate the design population, since small changes in right leg angle will not have large effects on hip height.

Helmet Contour

Helmet contours were calculated identically to the contours for FEP.

Knee Contour

Knee contours were calculated using the same methods applied to the FEP data.

Elbow Contour

Elbow contours were calculated using the same methods applied to the FEP data.

Accommodation Models for Driver in Highly Reclined Seating

Inputs

In addition to variables listed above for all models, the seat height (AHPZ to HARP) and the seat back angle (degrees from vertical of the lower support surface) were inputs to the HRS accommodation models. The origin is the HARP (X), seat centerline (Y), and floor, i.e., AHP (Z). Example calculations were conducted at the PPE ensemble level and with seat height of 150 mm (HARP above heel surface) and seat back angle of 40 degrees.

Outputs

Figure 29 shows sample contours and adjustment ranges generated by the accommodation models.

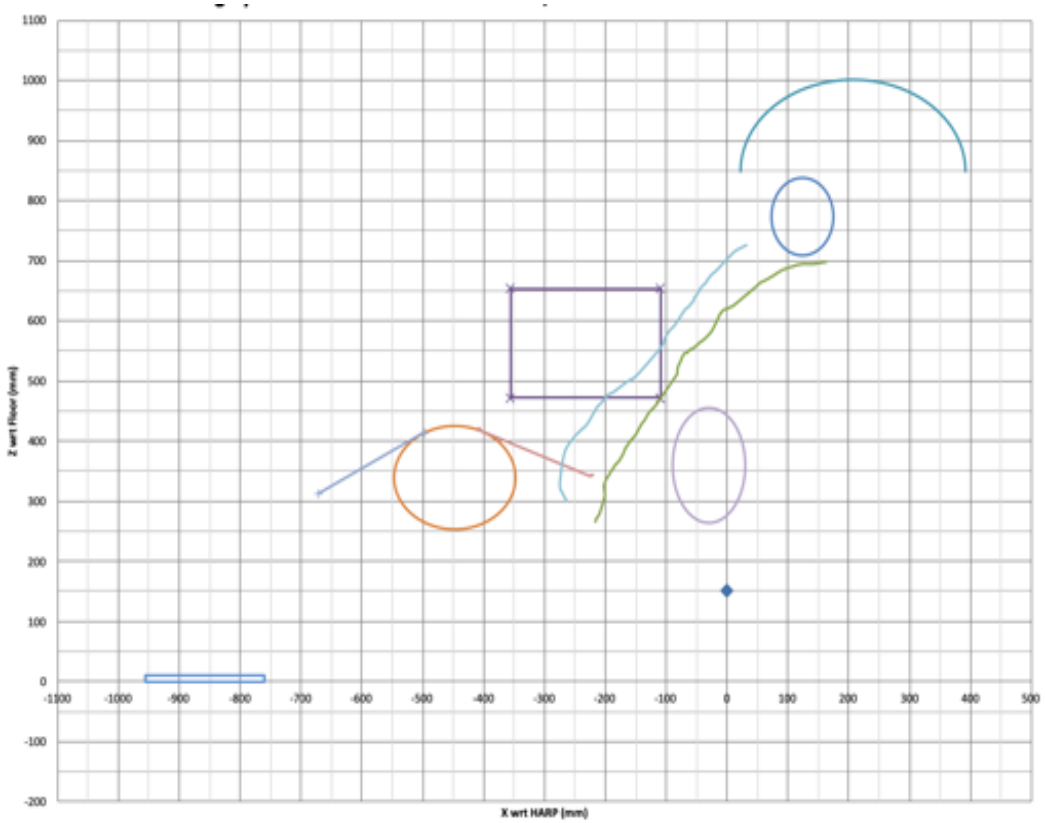

Figure 29. Side-view illustration of HRS accommodation contours.

Pedal Adjustment Range

The seat position was fixed, but the participants adjusted the fore-aft location of the foot rest surface (can also represent pedal locations) to a comfortable position. The fore-aft location of the heel point was modeled relative to HARP. Because the values were not affected by seat height, seat back angle, or ensemble level, they are modeled only as a

function of anthropometry. Consequently, the values are the same for any levels of the other factors.

Eyellipse

The eyellipse location was strongly affected by seat back angle and body dimensions and to a lesser extent the ensemble level. No correlation was observed between the X and Z eye location coordinates, so the eyellipse is square to grid (unlike the fixed-heel driver eyellipse). The vertical and fore-aft axis cutoffs are calculated independently to obtain axis lengths. The centroid is calculated at the midpoint of each axis. Although initially calculate with respect to HARP, the seat height was added to express the Z coordinate with respect to the floor (heel rest surface, i.e., AHPZ). Left and right eyellipses (Figure 30) were calculated assuming an interpupilary breadth of 65 mm.

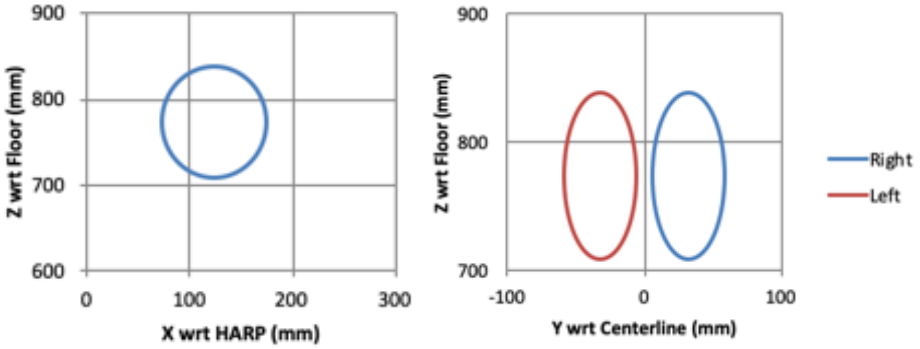

Figure 30. Eyellipses in side view (left) and rear view (right)

Helmet Contour

The helmet contour was constructed using the standard helmet model developed in prior work (Appendix C) positioned based on the forward, upper, and rearward extremes of the contour. This method is identical to the procedures used previously for squad helmet contours (Zerehsaz et al. 2014b). Specifically, the front of the contour is 52.2 mm forward of the front of the eyellipse; the top of the contour is 161.8 mm above the top of the eyellipse; and the rear of the contour is 217.1 mm aft of the rear of the eyellipse. The rear-view contours for the left and right eye are based on a helmet width of 259.8 mm, taking into account the interpupillary spacing of 65 mm. An additional 23 mm is added on each side for head turn.

Steering Yoke Position

The participants' preferred fore-aft steering yoke positions were affected by seat back angle as well as ensemble and ln(BMI). However, the vertical position was not significantly affected by any variables, so the mean value was a constant 413 mm above HARP in all conditions. The vertical range was computed using the observed standard deviation of 46.5 mm.

Elbow Contour

Elbow contours were calculated in the same manner as in the other mockups. All three coordinates were affected by the ensemble. Anthropometric variables and seat back angle were also important. The vertical extent was adjusted to account for the olecranon process and the left and right contours were centered on the seat centerline.

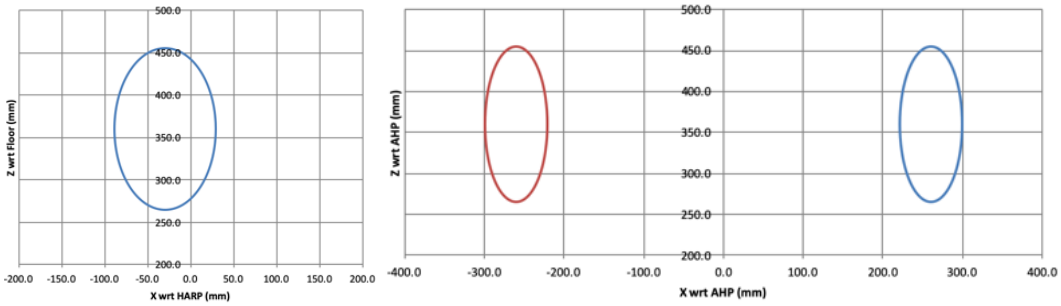

Figure 31. Elbow contours in side view (left) and rear view (right).

Knee Contours

The calculation procedure for the knee contours was identical to those used for the other driving conditions. The contours were expressed relative to HARP (X), seat centerline (Y), and the heel rest surface, i.e. floor or AHP (Z). The lateral extent was expanded based on the standard knee width estimate of 110 mm.

DISCUSSION

This report presents the first data-based posture prediction and accommodation models for atypical driver configurations for military vehicles. The data are based on a large, diverse sample of Soldiers, and the models were designed to be parametric so that they can represent a wide range of current and future warfighter populations. The new models include the effects of two ensemble levels added to the ACU level, which is similar to street clothing.

The driver configurations differ from those used in the previous study with fixed heel point in several ways:

- the current study used generic seating surfaces, rather than production seats;
- test conditions in the OOH configurations were adjusted based on participants' body dimensions;
- a yoke rather than a steering wheel was used, and participants demonstrated their preferred positioning (the steering wheel in the previous driver study was fixed in position);

Limitations and Future Work

These results are limited in several ways by the data collection environment and protocols. In addition to minimally contoured, artificial seats, the data were gathered during short-duration sitting sessions (a few minutes in each test condition), and the laboratory environment lacked many of the other spatial constraints of military vehicle. However, the goal of the current work was to establish the space requirements and adjustment preferences without those constraints for use in design. The conditions did not include a realistic driving task and no dynamic ride motion was simulated.

The fixed eye point was artificially constructed, without a realistic driving vision task. A particular remote-vision system could have less constraint, and no adjustability in the FEP was simulated. The HRS seat may not be representative of any particular vehicle seat intended for reclined conditions. The test seat had a two-piece back with the upper back component at a fixed angle to the lower back. The angle of the front of the seat cushion was adjusted for each seat height, but may have provided less thigh support than a more realistic seat. Similarly, the OOH seat was idealized, with an angled front of the cushion that might not be available in production seats.

The two most important limitations of the models are the unknown dependence on the clothing/gear ensembles and seats. Different body armor designs, for example with thicker or thinner plates, could affect torso posture and position. Seat design could also influence posture and position and could interact with the body armor design. Future research is needed to address these issues.

REFERENCES

Reed, M.P. and Ebert, S.M (2013). The Seated Soldier Study: Posture and Body Shape in Vehicle Seats. Technical Report UMTRI-2013-13. University of Michigan Transportation Research Institute, Ann Arbor, MI.

Gordon, C. C., Blackwell, C. L., Bradtmiller, B., Parham, J. L., Barrientos, P., Paquette, S. P., and Mucher, M. (2014). 2012 Anthropometric Survey of Marine Corps Personnel: Methods and Summary Statistics. (NATICK/TR-15/007). Army Natick Soldier Research Development and Engineering Center, Natick, MA.

Zerehsaz, Y., Ebert, S.M., and Reed, M.P. (2014a). Development of Accommodation Models for Soldiers in Vehicles: Driver. Technical Report UMTRI-2014-26. University of Michigan Transportation Research Institute, Ann Arbor, MI.

Zerehsaz, Y., Ebert, S.M., and Reed, M.P. (2014b). Development of Accommodation Models for Soldiers in Vehicles: Squad. Technical Report UMTRI-2014-39. University of Michigan Transportation Research Institute, Ann Arbor, MI.

APPENDIX A
PARTICIPANT INTERACTION SCRIPTS

Fixed-Eye-Point Station Instruction Script

Please have a seat in this mockup with your feet on this surface. Do NOT touch this box *(the vision target).* Adjust the back angle until you are comfortable. *Soldier adjusts.*

Now adjust the up-down and forward-backward until you see the two dashed lines again, but no green above or below them. *(Show printout)**

Move the pedals until the accelerator is in a comfortable position**. *Investigator moves the pedals 50 mm closer to the soldier.* Move the pedals again until the accelerator is in a comfortable position.

Now I would like you to position the steering yoke. Please adjust the up-down, in-out and tilt until you are comfortable and still can turn the yoke all the way to the side while maintaining your grip.

Now please take a look at the box again and make any small adjustments so that you see the two dashed lines again, but no green above or below them.

Check Soldier Posture

In a symmetrical posture (except for the legs)
Right foot on accelerator
Left foot flat on floor
Centered left-right in the seat
Both hands on the steering yoke
Looking in the FEP

Instruction Script for Fixed-Heel Condition (Seated Soldier Condition 5)

Please adjust the seat to a comfortable position for driving, as though you were going to be driving for a long time.

Adjust the back angle, seat position up-down and fore-aft.

OOH Instruction Script

This is a semi-standing seat. Please do not jump up onto it. Step on the platform and stand so your thighs are touching the seat. If you can bend your knees to sit, please do so, but do not jump up onto the seat.

Now, please position yourself comfortably so that your ankles are directly under your knees

Use your foot to position this accelerator pedal to a comfortable position.

Position the steering yoke. Please adjust the up-down, in-out and tilt until you are comfortable and can still turn the yoke all the way to the side (90˚) while maintaining your grip.

Adjust the part of the seat under your thighs until you feel comfortable.
Digitize posture

Now position the yoke again. However, this time place it in the lowest comfortable position
Digitize yoke position

Check Soldier Posture

In a symmetrical posture (except leg on accelerator)
Centered left-right in the seat
Sitting with the ankle directly below the knee
Both hands on the steering yoke
Looking forward as though driving
Can lean against seat back

APPENDIX B
GENERAL CALCULATION METHODS FOR ACCOMMODATION MODELS

This section closely follows presented previously (Zerehsaz et al 2014a, 2014b).

Convolving Normal Distributions with Linear Models

The data analysis and model development in this report are based on linear regression analysis and exploit some of the statistical characteristics of linear functions of variables that follow a normal distribution. In general, a dimension of interest, such as fore-aft seat position, is expressed as a linear function of potential predictors, such as seat height and driver stature. The models have the form

$$y = c_0 + c_1 x_1 + c_2 x_2 + ... + e(0, s^2) \quad [B1]$$

where y is the dependent measure to be predicted, the c_i are constant coefficients obtained by fitting to the data, the x_i are the predictors (vehicle and driver body dimensions). The final "error" term $e(0, s^2)$ is a random, normally distributed variable with zero mean and variance s^2, where s is the root mean square error (RMSE) of the regression. In computational terms, the RMSE is the standard deviation of the data vector that is obtained by subtracting the regression prediction from each data observation. This residual variance is a crucial part of the modeling in this report.

The model development procedure in this report exploits an important feature of normal distributions, which is that the mean and standard deviation of a linear function of a normal distribution is also a normal distribution. Specifically, if

$$Y = c_0 + c_1 X \quad [B2]$$

where c_0 and c_1 are constants and X is a normal distribution with mean X_{Mean} and standard deviation s_X, then Y is also a normal distribution, with mean

$$Y_{Mean} = c_0 + c_1 X_{Mean} \quad [B3]$$

and variance (standard deviation squared) of

$$s_Y^2 = (c_1 s_X)^2 \quad [B4]$$

The sum of two normal distributions is also a normal distribution, with variance equal to the sum of the variances. So, the residual variance from a regression can be included in estimating the distribution of the dependent measures. For example, consider

$$HARPX = c_0 + c_1 Stature + e(0, s^2) \quad [B5]$$

where *HARPX* is driver-selected fore-aft seat position, c_0 and c_1 are constant coefficients from the regression analysis, and s is the root mean square error from the regression. If stature is modeled as a normally distributed random variable, this becomes the sum of

two normally distributed random variables. Hence, for this example, *HARPX* is modeled as a normal distribution with mean

$$HARPX_{\text{Mean}} = c_0 + c_1\, Stature_{\text{Mean}} \quad \text{[B6]}$$

and variance

$$s_{\text{Stature}}^2 = (c_1\, s_{\text{Stature}})^2 \quad \text{[B7]}$$

This formulation is particularly valuable for modeling driver posture because the relevant human descriptors, such as stature and body mass index, are approximately normally distributed within gender or can be transformed to be. If the predictors are correlated, then the calculation of the variance of the independent is slightly different. For the equation

$$Y = c_1\, X_1 + c_2\, X_2 \quad \text{[B8]}$$

where X_1 and X_2 are normally distributed random variables with variances s_1^2 and s_2^2 and correlation $r_{1,2}$, the variance of Y is given by

$$s_Y^2 = (c_1\, s_1)^2 + (c_2\, s_2)^2 + 2\, r_{1,2}\, s_1\, s_2 \quad \text{[B9]}$$

For a difference between two normal random variables

$$Y = c_1\, X_1 - c_2\, X_2 \quad \text{[B10]}$$

the covariance ($r_{1,2}\, s_1\, s_2$) is subtracted:

$$s_Y^2 = (c_1\, s_1)^2 + (c_2\, s_2)^2 - 2\, r_{1,2}\, s_1\, s_2 \quad \text{[B11]}$$

In general, the occupant population includes both men and women. Although single-gender distributions of many anthropometric variables can be accurately approximated as normal distributions, the male and female components must usually be modeled separately. The level of accommodation for each gender is computed and the respective fractions are combined using the population gender mix. For example, if the fraction of males in the population is m, the total fraction accommodated is

$$F_{\text{total}} = m\, (F_{\text{m}}) + (1\text{-}m)\, F_{\text{f}} \quad \text{[B12]}$$

where F_{m} and F_{f} are the fractions of male and female occupants accommodated, respectively.

Cutoff Concept

To construct geometric contours that represent accommodation models, we want to identify "cutoff points" beyond which a desired percentage of the population lies. For example, we may want to construct a contour such that 95% of heads lie below a tangent to the contour. To identify cutoff points on each axis of interest, we calculate the mean and standard deviation of the individual male and female populations, then iteratively

find the location (an X, Y, or Z coordinate value) such that the combined population is appropriately divided at the cutoff point. Note that for a single-sex population approximated by a normal distribution we can immediately calculate the cutoff in closed form from the cumulative normal distribution, but for the combined population we must iterate, applying the male/female distribution (for example, 90% male).

Computing Cutoffs in Excel

The Excel spreadsheets accompanying this report use the function NORMDIST to model the combined male and female population distribution. The function representation of equation B12 is

```
=FractionMale*NORMDIST(cutoff_value, male_mean, male_standard_deviation, 1) + (1-
FractionMale)*NORMDIST(cutoff_value, female_mean, female_standard_deviation, 1)
```

where the means and standard deviations are the values computed for the distribution of interest (for example, front of seat track travel. The last argument to the NORMDIST function is a 1 to indicate that the cumulative function is to be used. The cutoff value is iterated using the Goal Seek functionality in Excel to achieve the desired percentage cutoff (e.g., 5% for 95% accommodation).

APPENDIX C

DRIVER ANTERIOR TORSO CONTOURS

All coordinates in mm.

Rifleman (ENC/BBG) Side View Relative to Reference Point

X	Z
210.7	269.7
201.3	262.2
193.1	254.7
187.7	246.2
186.5	245.1
180.1	234.3
171.6	219.9
163.8	209.3
158.7	198.6
157.9	195.5
150.9	184.4
148.4	175.9
143.9	166.2
144.1	164.9
144.2	164.6
143.5	161.1
137.0	149.1
133.0	144.3
121.4	115.3
115.7	106.1
109.7	90.7
107.9	77.6
77.5	22.3
64.6	8.9
58.4	2.2
56.0	-0.4
50.9	-6.8
43.5	-14.8
38.1	-18.5
34.4	-25.3
25.4	-40.6
23.8	-42.2
13.5	-73.3
4.5	-87.0
-3.2	-99.1
-12.7	-121.2
-14.1	-143.1
-14.1	-143.1
-12.7	-165.8
-9.9	-185.8
-2.8	-196.3
5.3	-206.3

Rifleman (ENC/BBG) Top View Relative to Reference Point (Z Value is -121 mm)

X	Y
157.3	401.9
147.2	400.3
128.1	389.4
125.2	386.0
110.4	367.3
100.0	355.8
39.2	291.0
31.8	281.2
17.4	260.7
4.1	239.9
-7.5	222.1
-9.5	212.3
-13.6	178.5
-13.4	177.6
-12.3	30.0
-19.4	5.1
-20.5	-2.2
-20.1	-10.6
-26.1	-33.1
-26.7	-39.1
-30.0	-65.3
-31.4	-72.7
-31.4	-72.7
-18.6	-106.6
-13.1	-120.3
8.5	-138.4
23.3	-143.5
58.9	-165.9
65.9	-169.3
76.0	-174.7
95.9	-187.1
103.5	-194.7
107.6	-197.4
138.3	-220.7
169.1	-239.3
183.4	-244.6

IOTV Side View Relative to Reference Point (PPE Ensemble Level)

X	Z
-138.3	-344.8
-137.9	-344.3
-137.3	-338.9
-135.2	-334.4
-133.8	-329.3
-131.1	-298.7
-132.0	-296.4
-133.3	-292.7
-134.1	-289.6
-134.7	-288.1
-136.1	-284.5
-135.6	-280.4

-135.7	-280.0
-135.3	-276.6
-134.0	-271.7
-133.7	-269.7
-132.6	-267.3
-131.7	-266.1
-130.1	-260.0
-129.8	-259.8
-125.1	-248.0
-124.9	-246.4
-120.0	-239.2
-116.0	-228.0
-115.7	-227.0
-113.5	-214.8
-113.1	-214.8
-108.5	-203.5
-107.5	-201.1
-101.2	-190.1
-97.8	-178.3
-94.5	-168.8
-92.4	-165.7
-91.6	-163.6
-89.7	-157.0
-89.1	-155.8
-87.1	-149.6
-85.0	-146.9
-82.0	-141.3
-81.7	-140.8
-80.1	-139.9
-79.8	-139.2
-54.4	-78.7
-54.7	-75.6
-55.4	-70.1
-54.7	-62.9
-53.5	-58.8
-53.0	-57.7
-52.2	-51.1
-50.2	-44.4
-48.9	-42.1
-47.8	-41.5
-45.3	-40.6
-41.8	-35.1
-38.7	-33.1
-36.1	-30.4
-33.3	-27.4
-31.0	-24.1
-26.8	-18.3
-25.8	-17.9
-19.0	-8.9
-11.8	5.0
-4.7	33.4
-3.7	34.8
-3.0	35.6
-1.2	39.5
3.3	43.3
3.5	43.4
5.3	43.6
12.0	49.3

13.3	49.8
46.4	91.5
47.6	94.1
48.4	95.3
50.1	97.0
53.1	99.1
54.0	99.8
55.1	100.8
57.6	102.4
63.2	107.5
66.1	110.1
68.2	111.9
70.9	114.6
75.6	119.3
80.3	123.4
85.5	127.2
89.2	129.6
94.0	132.0
94.8	132.5
99.5	135.0
101.9	136.7
109.5	139.7
115.1	141.4
118.8	142.0
126.6	143.6
127.3	143.4
149.4	151.8

IOTV Top View Relative to Reference Point (PPE Ensemble Level)

X	Y	Z
58.7	-198.7	-250
48.9	-197.6	-250
48.3	-198.0	-250
45.2	-197.4	-250
36.3	-196.4	-250
34.0	-195.6	-250
28.2	-194.2	-250
27.6	-194.2	-250
22.2	-191.5	-250
16.3	-190.0	-250
15.8	-190.2	-250
12.1	-189.0	-250
10.1	-188.7	-250
1.7	-186.4	-250
-0.6	-185.9	-250
-1.5	-185.3	-250
-4.8	-183.8	-250
-6.1	-183.5	-250
-14.2	-181.8	-250
-18.7	-180.4	-250
-25.5	-178.0	-250
-32.1	-174.8	-250
-34.9	-174.2	-250
-40.3	-171.4	-250
-48.4	-168.0	-250
-51.7	-167.0	-250

-52.8	-166.4	-250
-57.9	-163.8	-250
-63.6	-161.2	-250
-66.9	-159.9	-250
-71.8	-156.7	-250
-75.8	-154.2	-250
-79.5	-153.0	-250
-86.6	-149.2	-250
-88.5	-148.2	-250
-90.7	-147.0	-250
-91.7	-146.1	-250
-92.5	-144.8	-250
-94.1	-141.9	-250
-95.2	-139.0	-250
-95.4	-137.7	-250
-95.7	-134.9	-250
-96.9	-131.4	-250
-96.9	-130.2	-250
-97.3	-123.4	-250
-105.7	-97.8	-250
-109.2	-89.1	-250
-111.7	-79.3	-250
-112.3	-77.2	-250
-113.0	-73.0	-250
-115.4	-63.9	-250
-115.4	-57.5	-250
-116.8	-52.1	-250
-118.2	-46.2	-250
-119.1	-37.8	-250
-120.1	-34.6	-250
-121.3	-25.8	-250
-121.7	-23.2	-250
-123.3	-16.8	-250
-122.9	-11.9	-250
-124.0	-6.5	-250
-124.4	-5.1	-250
-126.6	2.0	-250
-126.6	8.2	-250
-126.9	10.7	-250
-126.4	17.5	-250
-127.3	24.8	-250
-127.0	26.8	-250
-127.0	28.3	-250
-126.7	44.4	-250
-127.2	46.5	-250
-126.8	47.7	-250
-126.3	58.9	-250
-125.1	67.0	-250
-125.1	67.0	-250
-121.9	76.8	-250
-119.7	80.3	-250
-116.7	85.4	-250
-116.6	86.1	-250
-115.2	90.1	-250
-115.1	90.4	-250
-115.1	90.8	-250
-113.5	94.4	-250
-112.3	99.9	-250

-108.7	107.9	-250
-108.4	110.5	-250
-107.0	113.1	-250
-105.4	117.7	-250
-102.6	122.4	-250
-89.4	160.9	-250
-89.0	163.7	-250
-88.8	166.4	-250
-89.3	168.3	-250
-88.2	171.0	-250
-84.7	176.9	-250
-82.8	178.5	-250
-78.9	180.3	-250
-75.8	182.2	-250
-75.3	182.6	-250
-70.4	183.7	-250
-64.2	186.4	-250
-57.8	188.6	-250
-54.9	189.9	-250
-53.8	190.2	-250
-51.1	191.1	-250
-50.2	191.4	-250
-39.6	195.5	-250
-33.7	197.8	-250
-25.3	200.8	-250
-23.6	201.0	-250
-19.1	202.8	-250
-6.5	207.3	-250
0.4	209.0	-250
11.1	211.0	-250
15.5	213.2	-250
24.1	215.7	-250
34.9	218.7	-250
35.2	218.7	-250
38.6	218.8	-250
41.8	219.4	-250

APPENDIX D

HELMET CONTOURS

Relative to Eye and Head Centerline

Sagittal		Coronal	
X	Z	Y	Z
-52.2	53.4	-129.9	-11.0
-51.8	56.7	-129.0	-5.3
-51.2	60.0	-128.1	0.2
-50.6	63.3	-127.2	5.7
-50.0	66.4	-126.3	10.9
-49.3	69.5	-125.4	16.1
-48.6	72.5	-124.5	21.1
-47.8	75.5	-123.5	25.9
-47.0	78.4	-122.6	30.6
-46.1	81.2	-121.7	35.2
-45.2	83.9	-120.7	39.7
-44.3	86.6	-119.8	44.0
-43.3	89.2	-118.8	48.2
-42.3	91.8	-117.9	52.3
-41.3	94.3	-116.9	56.3
-40.2	96.7	-115.9	60.1
-39.0	99.1	-114.9	63.8
-37.9	101.4	-113.9	67.5
-36.7	103.7	-112.9	71.0
-35.4	105.9	-111.9	74.4
-34.2	108.1	-110.9	77.7
-32.9	110.2	-109.9	80.9
-31.5	112.2	-108.9	84.0
-30.2	114.2	-107.8	87.0
-28.8	116.2	-106.8	89.9
-27.3	118.0	-105.8	92.8
-25.9	119.9	-104.7	95.5
-24.4	121.7	-103.6	98.1
-22.9	123.4	-102.6	100.7
-21.3	125.1	-101.5	103.2
-19.8	126.7	-100.4	105.6
-18.2	128.3	-99.3	107.9
-16.6	129.9	-98.2	110.1
-14.9	131.4	-97.1	112.3
-13.3	132.8	-96.0	114.4
-11.6	134.2	-94.8	116.4
-9.9	135.6	-93.7	118.3
-8.2	136.9	-92.6	120.2

-6.4	138.2	-91.4	122.0
-4.6	139.5	-90.3	123.7
-2.9	140.7	-89.1	125.4
-1.0	141.8	-87.9	127.1
0.8	143.0	-86.8	128.6
2.6	144.0	-85.6	130.1
4.5	145.1	-84.4	131.6
6.4	146.1	-83.2	133.0
8.2	147.1	-82.0	134.3
10.2	148.0	-80.7	135.6
12.1	148.9	-79.5	136.9
14.0	149.8	-78.3	138.0
16.0	150.6	-77.0	139.2
17.9	151.4	-75.8	140.3
19.9	152.2	-74.5	141.4
21.9	152.9	-73.3	142.4
23.9	153.6	-72.0	143.4
25.9	154.3	-70.7	144.3
27.9	154.9	-69.4	145.2
29.9	155.5	-68.1	146.1
31.9	156.1	-66.8	146.9
34.0	156.6	-65.5	147.7
36.0	157.1	-64.2	148.5
38.1	157.6	-62.9	149.2
40.1	158.1	-61.5	149.9
42.2	158.5	-60.2	150.6
44.2	158.9	-58.9	151.2
46.3	159.3	-57.5	151.8
48.4	159.6	-56.2	152.4
50.5	159.9	-54.8	152.9
52.5	160.2	-53.4	153.5
54.6	160.5	-52.0	154.0
56.7	160.7	-50.6	154.5
58.8	160.9	-49.3	155.0
60.9	161.1	-47.9	155.4
63.0	161.3	-46.4	155.8
65.1	161.4	-45.0	156.2
67.1	161.6	-43.6	156.6
69.2	161.6	-42.2	157.0
71.3	161.7	-40.8	157.3
73.4	161.8	-39.3	157.7
75.5	161.8	-37.9	158.0
77.6	161.8	-36.4	158.3
79.6	161.8	-35.0	158.6
81.7	161.7	-33.5	158.8
83.8	161.7	-32.0	159.1

85.8	161.6	-30.6	159.3
87.9	161.5	-29.1	159.6
89.9	161.4	-27.6	159.8
92.0	161.2	-26.1	160.0
94.0	161.1	-24.6	160.2
96.0	160.9	-23.1	160.4
98.1	160.7	-21.6	160.5
100.1	160.4	-20.1	160.7
102.1	160.2	-18.6	160.8
104.1	159.9	-17.1	161.0
106.1	159.6	-15.6	161.1
108.0	159.3	-14.1	161.2
110.0	159.0	-12.5	161.3
112.0	158.7	-11.0	161.4
113.9	158.3	-9.5	161.5
115.9	157.9	-7.9	161.6
117.8	157.5	-6.4	161.7
119.7	157.1	-4.8	161.7
121.6	156.6	-3.3	161.8
123.5	156.2	-1.7	161.8
125.4	155.7	-0.2	161.8
127.3	155.2	1.4	161.8
129.1	154.7	3.0	161.8
131.0	154.2	4.5	161.8
132.8	153.6	6.1	161.8
134.6	153.0	7.6	161.8
136.4	152.4	9.2	161.7
138.2	151.8	10.8	161.7
139.9	151.2	12.4	161.6
141.7	150.5	13.9	161.5
143.4	149.9	15.5	161.4
145.2	149.2	17.1	161.3
146.9	148.5	18.7	161.2
148.6	147.7	20.2	161.0
150.2	147.0	21.8	160.9
151.9	146.2	23.4	160.7
153.5	145.4	25.0	160.5
155.2	144.6	26.6	160.3
156.8	143.8	28.1	160.1
158.4	143.0	29.7	159.8
159.9	142.1	31.3	159.6
161.5	141.2	32.9	159.3
163.0	140.3	34.4	159.0
164.5	139.3	36.0	158.7
166.0	138.4	37.6	158.3
167.5	137.4	39.2	157.9

169.0	136.4	40.7	157.5
170.4	135.4	42.3	157.1
171.8	134.4	43.9	156.7
173.2	133.3	45.4	156.2
174.6	132.2	47.0	155.7
175.9	131.1	48.5	155.2
177.3	130.0	50.1	154.6
178.6	128.8	51.6	154.0
179.9	127.6	53.2	153.4
181.2	126.4	54.7	152.7
182.4	125.2	56.2	152.0
183.7	123.9	57.8	151.3
184.9	122.6	59.3	150.5
186.1	121.3	60.8	149.7
187.2	120.0	62.3	148.8
188.4	118.6	63.8	147.9
189.5	117.3	65.4	147.0
190.6	115.8	66.9	146.0
191.7	114.4	68.3	145.0
192.8	112.9	69.8	143.9
193.8	111.4	71.3	142.8
194.8	109.9	72.8	141.6
195.8	108.3	74.2	140.4
196.8	106.7	75.7	139.1
197.7	105.1	77.1	137.8
198.6	103.5	78.6	136.4
199.5	101.8	80.0	134.9
200.4	100.1	81.4	133.4
201.3	98.3	82.9	131.8
202.1	96.6	84.3	130.2
202.9	94.7	85.7	128.5
203.7	92.9	87.0	126.7
204.5	91.0	88.4	124.9
205.2	89.1	89.8	123.0
206.0	87.1	91.1	121.0
206.7	85.2	92.5	118.9
207.3	83.1	93.8	116.8
208.0	81.1	95.1	114.6
208.6	79.0	96.4	112.3
209.2	76.8	97.7	109.9
209.8	74.6	99.0	107.5
210.4	72.4	100.3	104.9
210.9	70.2	101.5	102.3
211.4	67.9	102.8	99.5
211.9	65.5	104.0	96.7
212.4	63.1	105.2	93.8

212.8	60.7	106.4	90.7
213.2	58.2	107.6	87.6
213.6	55.7	108.8	84.4
214.0	53.1	109.9	81.1
214.4	50.5	111.0	77.6
214.7	47.9	112.2	74.1
215.0	45.2	113.3	70.4
215.3	42.4	114.3	66.6
215.6	39.6	115.4	62.7
215.8	36.8	116.5	58.7
216.0	33.8	117.5	54.6
216.2	30.9	118.5	50.3
216.4	27.9	119.5	45.9
216.6	24.8	120.5	41.4
216.7	21.7	121.4	36.7
216.8	18.5	122.4	31.9
216.9	15.3	123.3	27.0
217.0	12.0	124.2	21.9
217.0	8.7	125.1	16.7
217.0	5.3	125.9	11.3
217.1	1.8	126.7	5.8
217.0	-1.7	127.6	0.1
217.0	-5.3	128.3	-5.7
216.9	-8.9	129.1	-11.7